Vibration and buckling analysis of functionally graded sandwich plates with improved transverse shear stiffness based on the first-order shear deformation theory

Trung-Kien Nguyen *[1], Thuc P. Vo[2], and Huu-Tai Thai[3]

[1]*Faculty of Civil Engineering and Applied Mechanics, University of Technical Education Ho Chi Minh City, 1 Vo Van Ngan Street, Thu Duc District, Ho Chi Minh City, Vietnam*

[2]*Faculty of Engineering and Environment, Northumbria University, Newcastle upon Tyne, NE1 8ST, UK.*

[3]*School of Civil and Environmental Engineering, The University of New South Wales, NSW 2052, Australia.*

December 9, 2013

Abstract

An improved transverse shear stiffness for vibration and buckling analysis of functionally graded sandwich plates based on the first-order shear deformation theory is proposed in this paper. The transverse shear stress obtained from the in-plane stress and equilibrium equation allows to derive analytically an improved transverse shear stiffness and associated shear correction factor of the functionally graded sandwich plate. Sandwich plates with functionally graded faces and both homogeneous hardcore and softcore are considered. The material property is assumed to be isotropic at each point and vary through the plate thickness according to a power-law distribution of the volume fraction of the constituents. Equations of motion and boundary conditions are derived from Hamilton's principle. The Navier-type solutions are obtained for simply-supported boundary conditions, and exact formulas are proposed and compared with the existing solutions to verify the validity of the developed model. Numerical results are obtained for simply-supported functionally graded sandwich plates made of three sets of material combinations of metal and ceramic: Al/Al_2O_3, Al/SiC, and Al/WC to investigate the effects of the power-law index, thickness ratio of

*Corresponding author: tel.: +84 (8) 38972092; E-mail address: ntkien@hcmute.edu.vn

layer, material contrast on the shear correction factors, natural frequencies and critical buckling loads as well as load-frequency curves.

Keywords: Functionally graded sandwich plates; Buckling; Vibration; Load-frequency curves.

1 Introduction

Sandwich structures are a class of composite materials in that they have a core material is bonded to, and faced with a skin material. These structures are used in a wide variety of applications including aircraft, aerospace, naval/marine, construction, and transportation industries where strong stiff and light structures are required. Practically however, due to the mismatch of properties between the face sheets and the core, stress concentrations can occur at these interfaces, often leading to delamination, which is a major concern[1,2]. To overcome this problem, the concept of functionally graded (FG) sandwich structure is proposed. This structure can be categorized into two classes: FG facesheet homogeneous core and homogeneous facesheet FG core.

Due to increasing of FG material applications in engineering fields, many computational models have been developed for predicting the response of FG plates. The classical plate theory (CPT) has been used for buckling and vibration analysis of FG thin plates[3–8]. However, for moderately thick plates, it overestimates buckling loads and natural frequencies due to the neglecting the transverse shear deformation effect. The first-order shear deformation theory (FSDT) accounts for the transverse shear deformation effect, but requires a shear correction factor to correct the shear stress and force[9–14]. To overcome this adversity, many higher-order shear deformation plate theories (HSDTs) have been proposed based on the assumption of higher-order variations of displacements[15–27]. Although the shear stresses are refined through the thickness direction in HSDTs, their equations of motion are much more complicated than those of FSDT due to involving higher-order terms.

Although there are several research works reported on FG plates, the studies on buckling and vibration of FG sandwich plates are few in number, most of which used the HSDTs. The sinusoidal shear deformation theory was applied by Zenkour[28] for buckling and free vibration of a simply supported FG sandwich plate. Li et al.[29] proposed a three-dimensional (3D) vibration analysis of FG sandwich plates with FG faces and both homogeneous hardcore and softcore. Meiche et al.[30] proposed a FG sandwich plate model for buckling and vibration using a new hyperbolic shear deformation theory. Based on a new four variable refined plate theory, Bourada et al.[31] considered the thermal buckling of FG sandwich plates. Xiang et al.[32] used a n-order shear deformation theory for free vibration of FG and composite sandwich plates. Natarajan and Manickam[33] proposed an accurate theory for

bending and vibration of FG sandwich plates in which two common types of FG sandwich plates were considered. Neves et al.[34] studied static, free vibration and buckling behaviour of isotropic and sandwich functionally graded plates using a quasi-3D higher-order shear deformation theory and a meshless technique.

This paper, which is extended from the previous works[35,36], aims to study vibration and buckling analysis of functionally graded sandwich plates with improved transverse shear stiffness based on the FSDT. Here, the transverse shear stress is derived from expression of the in-plane stress and equilibrium equation and thus, its improved shear stiffness is then obtained analytically. Sandwich plates with FG faces and both homogeneous hardcore and softcore are considered. The material property is assumed to be isotropic at each point and vary through the plate thickness according to a power law distribution of the volume fraction of the constituents. Equations of motion and boundary conditions are derived from Hamilton's principle. The Navier-type solutions are obtained for simply-supported boundary conditions, and exact formulas are proposed and compared with the existing solutions to verify the validity of the developed theory. Numerical results are obtained for simply-supported FG sandwich plates made of three sets of material combinations of metal and ceramic: Al/Al_2O_3, Al/SiC, and Al/WC to investigate the effects of the power-law index, thickness ratio of layer, material contrast on the shear correction factors, natural frequencies and critical buckling loads as well as load-frequency curves.

2 Problem formulation

Consider a three-layer sandwich plate as in Figure 1. The face layers are made of a ceramic-metal isotropic material whose properties vary smoothly through the thickness according to the volume fractions of the constituents. The core layer is constituted by an isotropic homogeneous material. The vertical positions of the bottom and top surfaces, and of two interfaces between the layers are denoted by $h_0 = -\frac{h}{2}$, h_1, h_2, $h_3 = \frac{h}{2}$, respectively. Here, h is the plate thickness, h_1, h_2 vary according the thickness ratio of layers, $e_c = h_2 - h_1$ is the core thickness, $e_{ft} = h_3 - h_2$, $e_{fb} = h_1 - h_0$ the thicknesses of top and bottom face, respectively. All formulations are performed under the assumption of a linear elastic behaviour and small deformations of materials. The gravity is not taken into account. The Greek indices are assumed to range within {1,2} while the Latin indices take values {1,2,3}.

2.1 Effective material properties

The Voigt's model[37] is used to calculate the effective material properties of FG sandwich plates according to the power-law form. The mixture of the two materials according to the Voigt's model through the plate thickness is given by:

$$P^{(j)}(z) = (P_b - P_t)V_b^{(j)}(z) + P_t \tag{1}$$

where P_t and P_b are the Young's moduli (E), mass densities (ρ) of materials located at the top and bottom surfaces, and at the core of the plate, respectively, the volume fraction function $V_b^{(j)}$ defined by the power law as follows:

$$\begin{cases} V_b^{(1)}(z) = \left(\frac{z-h_o}{h_1-h_0}\right)^p & \text{for} \quad z \in [h_0, h_1] \\ \\ V_b^{(2)}(z) = 1 & \text{for} \quad z \in [h_1, h_2] \\ \\ V_b^{(3)}(z) = \left(\frac{z-h_3}{h_2-h_3}\right)^p & \text{for} \quad z \in [h_2, h_3] \end{cases} \tag{2}$$

where p is a power-law index, which is positive. Distribution of material with V_b through the plate thickness according to the power-law form for six cases of the thickness ratio of layer is presented in Figure 2.

2.2 Improved transverse shear stiffness

The displacement field of the FSDT is given by the following expressions:

$$\begin{aligned} u_\alpha(x, y, z) &= u_{o\alpha}(x, y, z) + z\theta_\alpha(x, y, z) \\ w_\alpha(x, y, z) &= w_{o\alpha}(x, y, z) \end{aligned} \tag{3}$$

where $u_{o\alpha}$, θ_α are the membrane displacements and rotations, $w_{o\alpha}$ denotes the transverse displacement of the plate. The membrane strains and in-plane stresses are related by the constitutive equation:

$$\sigma_{\alpha\beta}^{(j)}(x, y, z) = \bar{Q}_{\alpha\beta\gamma\delta}^{(j)}(z)(\epsilon_{\gamma\delta}^o(x, y) + z\chi_{\gamma\delta}(x, y)) \tag{4}$$

where $\bar{Q}_{\alpha\beta\gamma\delta}^{(j)}(z)$ are the components of the reduced elasticity tensor of the jth-layer at location z, $\epsilon_{\gamma\delta}^o$, $\chi_{\gamma\delta}$ are the membrane strains and curvatures of the plate, respectively. They are related with the membrane displacements $u_{o\alpha}$ and rotations θ_α as follows: $\epsilon_{\alpha\beta}^o(x, y) = \frac{1}{2}(u_{o\alpha,\beta} + u_{o\beta,\alpha})(x, y)$, $\chi_{\alpha\beta}(x, y) = \frac{1}{2}(\theta_{\alpha,\beta} + \theta_{\beta,\alpha})(x, y)$ where the comma indicates partial differentiation with respect to the

coordinate subscript that follows. Moreover, the generalized stresses ($N_{\alpha\beta}$, $M_{\alpha\beta}$) are associated to the in-plane stresses $\sigma^{(j)}_{\alpha\beta}$:

$$N_{\alpha\beta}(x,y) = \sum_{j=1}^{3} \int_{-h/2}^{h/2} \sigma^{(j)}_{\alpha\beta}(x,y,z)\, dz, \quad M_{\alpha\beta}(x,y) = \sum_{j=1}^{3} \int_{-h/2}^{h/2} z\sigma^{(j)}_{\alpha\beta}(x,y,z)\, dz \tag{5}$$

That leads to the constitutive equations of the FG sandwich plates:

$$\begin{aligned} N_{\alpha\beta}(x,y) &= A_{\alpha\beta\gamma\delta}\, \epsilon^{o}_{\gamma\delta}(x,y) + B_{\alpha\beta\gamma\delta}\, \chi_{\gamma\delta}(x,y) \\ M_{\alpha\beta}(x,y) &= B_{\alpha\beta\gamma\delta}\, \epsilon^{o}_{\gamma\delta}(x,y) + D_{\alpha\beta\gamma\delta}\, \chi_{\gamma\delta}(x,y) \end{aligned} \tag{6}$$

where ($A_{\alpha\beta\gamma\delta}$, $B_{\alpha\beta\gamma\delta}$, $D_{\alpha\beta\gamma\delta}$) are the stiffnesses of the FG sandwich plates given by:

$$(A_{\alpha\beta\gamma\delta}, B_{\alpha\beta\gamma\delta}, D_{\alpha\beta\gamma\delta}) = \sum_{j=1}^{3} \int_{-h/2}^{h/2} (1, z, z^2) \bar{Q}^{(j)}_{\alpha\beta\gamma\delta}(z) dz \tag{7}$$

The inversion of Eq. (6) enables to derive the membrane strains according to the generalized stresses as follows:

$$\begin{aligned} \epsilon^{o}_{\alpha\beta}(x,y) &= a_{\alpha\beta\gamma\delta} N_{\gamma\delta}(x,y) + b_{\alpha\beta\gamma\delta} M_{\gamma\delta}(x,y) \\ \chi_{\alpha\beta}(x,y) &= b_{\alpha\beta\gamma\delta} N_{\gamma\delta}(x,y) + d_{\alpha\beta\gamma\delta} M_{\gamma\delta}(x,y) \end{aligned} \tag{8}$$

where $(a_{\alpha\beta\gamma\delta}, b_{\alpha\beta\gamma\delta}, d_{\alpha\beta\gamma\delta})$ are the components of the compliance matrix. The matrices $\bar{Q}, A, B, D, a, b$ and d can be explicitly expressed in terms of the functions $E^{(j)}(z)$ and $\nu^{(j)}(z)$ describing the Young's modulus and the Poisson's ratio of the jth-layer at z, respectively. Moreover, it appears that the matrix b is symmetric owing to the fact that the material properties are isotropic. Substituting Eq. (8) into Eq. (4) leads to:

$$\sigma^{(j)}_{\alpha\beta}(x,y,z) = n^{(j)}_{\alpha\beta\gamma\delta}(z) N_{\gamma\delta}(x,y) + m^{(j)}_{\alpha\beta\gamma\delta}(z) M_{\gamma\delta}(x,y) \tag{9}$$

where $n^{(j)}_{\alpha\beta\gamma\delta}(z), m^{(j)}_{\alpha\beta\gamma\delta}(z)$ are the components of the localization tensors that are expressed as:

$$\begin{aligned} n^{(j)}_{\alpha\beta\gamma\delta}(z) &= \bar{Q}^{(j)}_{\alpha\beta\varepsilon\varphi}(z)(a_{\varepsilon\varphi\gamma\delta} + z b_{\varepsilon\varphi\gamma\delta}) \\ m^{(j)}_{\alpha\beta\gamma\delta}(z) &= \bar{Q}^{(j)}_{\alpha\beta\varepsilon\varphi}(z)(b_{\varepsilon\varphi\gamma\delta} + z d_{\varepsilon\varphi\gamma\delta}) \end{aligned} \tag{10}$$

Furthermore, it is well known that the calculation of the transverse shear stresses from the constitutive equations is not realistic because of the assumption of a constant shear strain through the plate thickness, the transverse shear stresses should be derived from the equilibrium equations:

$$\sigma^{(j)}_{\alpha 3} = -\int_{-h/2}^{z} \sigma^{(j)}_{\alpha\beta,\beta}\, dz \tag{11}$$

where the integration coefficients are selected to satisfy the boundary condition for shear stresses at the upper and lower surfaces of the plate. Substitution Eq. (9) into Eq. (11) conducts to the following relationship:

$$\sigma^{(j)}_{\alpha 3}(x,y,z) = \tilde{n}^{(j)}_{\alpha\beta\gamma\delta}(z) N_{\gamma\delta,\beta}(x,y) + \tilde{m}^{(j)}_{\alpha\beta\gamma\delta}(z) M_{\gamma\delta,\beta}(x,y) \tag{12}$$

where,

$$\begin{aligned}
&\tilde{n}^{(j)}_{\alpha\beta\gamma\delta}(z) = -\int_{-h/2}^{z} \bar{Q}^{(j)}_{\alpha\beta\varepsilon\varphi}(\xi)\left[a_{\varepsilon\varphi\gamma\delta} + \xi b_{\varepsilon\varphi\gamma\delta}\right] d\xi \\
&\tilde{m}^{(j)}_{\alpha\beta\gamma\delta}(z) = -\int_{-h/2}^{z} \bar{Q}^{(j)}_{\alpha\beta\varepsilon\varphi}(\xi)\left[b_{\varepsilon\varphi\gamma\delta} + \xi d_{\varepsilon\varphi\gamma\delta}\right] d\xi \\
&\tilde{n}^{(j)}_{\alpha\beta\gamma\delta} = \tilde{n}^{(j)}_{\gamma\delta\alpha\beta} = \tilde{n}^{(j)}_{\beta\alpha\gamma\delta}, \quad \tilde{m}^{(j)}_{\alpha\beta\gamma\delta} = \tilde{m}^{(j)}_{\gamma\delta\alpha\beta} = \tilde{m}^{(j)}_{\beta\alpha\gamma\delta}.
\end{aligned} \tag{13}$$

Using the equilibrium equations of the plate ($M_{\alpha\beta,\beta} - Q_\alpha = 0$, $N_{\alpha\beta,\beta} = 0$), neglecting the weak terms: $M_{22,1}$, $M_{11,2}$, $M_{12,1}$, $M_{12,2}$, and omitting the derivative effect of the membrane resultants, the transverse shear stresses given in Eq. (12) can be simplified as follows in the Cartesian coordinate system (x, y, z):

$$\begin{aligned}
\sigma^{(j)}_{xz}(x,z) &= \tilde{m}^{(j)}_{1111}(z) Q_x(x) \\
\sigma^{(j)}_{yz}(x,z) &= \tilde{m}^{(j)}_{2222}(z) Q_y(x)
\end{aligned} \tag{14}$$

Eq. (14) corresponds to two assumptions of cylindrical flexion around the $y-$ and $x-$axis[38]. It should be noted that $\tilde{m}^{(j)}_{1111}(z) = \tilde{m}^{(j)}_{2222}(z)$ due to the isotropic properties of materials. In practice, Eq. (14) is very often used to compute the shear stress of homogeneous plates with a quadratic form of $\tilde{m}^{(j)}_{1111}(z)$ and $\tilde{m}^{(j)}_{2222}(z)$, especially when commercial finite element packages are used. Moreover, the consideration of the balance of the transverse shear strain energy[35] by taking into account the shear stresses in Eq. (14) allows to derive the expression of an improved transverse shear stiffness for FG sandwich plates ($H_{44} = H_{55} = H$):

$$H = \left(\sum_{j=1}^{3} \int_{-h/2}^{h/2} \frac{\left[\tilde{m}^{(j)}_{1111}(z)\right]^2}{G^{(j)}(z)} dz \right)^{-1} \tag{15}$$

where $G^{(j)}(z) = E^{(j)}(z)/2[1+\nu^{(j)}(z)]$ is the shear modulus of the jth-layer at location z and there is no coupling between the shear strains in two directions ($H_{45} = 0$). Moreover, it is well-known that the FSDT plate models require an appropriate shear correction factor to calculate the transverse shear force. The discussion of this topic for the plates can be found in Berthelot[39] and Stefanos[40]. Taking into account Eq. (15), the shear correction factor ($\kappa_{44} = \kappa_{55} = \kappa$) is given by:

$$\kappa = \left(\sum_{j=1}^{3} \int_{-h/2}^{h/2} G^{(j)}(z)\, dz \right)^{-1} \left(\sum_{j=1}^{3} \int_{-h/2}^{h/2} \frac{\left[\tilde{m}^{(j)}_{1111}(z)\right]^2}{G^{(j)}(z)} dz \right)^{-1} \tag{16}$$

where it takes the five-sixth value for homogeneous plates. However, Eq. (16) shows that the shear correction factor depends on the material properties of FG through the plate thickness. Moreover, the use of the improved shear stiffnesses in Eq. (15) can provide a better evaluation of transverse shear forces.

2.3 Motion equations of FG sandwich plates

The differential equations of dynamic equilibrium of the FG sandwich plates without transverse loads can be derived from Hamilton principle as follows:

$$\begin{aligned} N_{\alpha\beta,\beta} &= I_0\ddot{u}_{o\alpha} + I_1\ddot{\theta}_\alpha \\ M_{\alpha\beta,\beta} - Q_\alpha &= I_1\ddot{u}_{o\alpha} + I_2\ddot{\theta}_\alpha \\ Q_{\alpha,\alpha} + \hat{N}_{\alpha\beta}w_{o,\alpha\beta} &= I_0\ddot{w}_o \end{aligned} \tag{17}$$

where the over dot indicates partial differentiation with respect to time. The inertia terms I_0, I_1, I_2 are expressed by:

$$(I_0, I_1, I_2) = \sum_{j=1}^{3}\int_{-h/2}^{h/2}(1, z, z^2)\rho^{(j)}(z)dz \tag{18}$$

Substitution of Eq. (6) into Eq. (17) by noticing that $Q_\alpha = H_{\alpha\beta}(w_{o,\beta} + \theta_\beta)$ with $H_{\alpha\beta} = H_{ij}$ $(i, j = 4, 5)$, leads to the differential equations of motion of FG sandwich plates:

$$\left(\mathbf{K}^{st} + \mathbf{K}^{g}\right)\mathbf{U} - \mathbf{M}\ddot{\mathbf{U}} = 0 \tag{19}$$

where $\mathbf{U}^T$=$\{u_{o\alpha},\, \theta_\alpha,\, w_{o\alpha}\}$ is the displacement vector and $\ddot{\mathbf{U}}^T$=$\{\ddot{u}_{o\alpha},\, \ddot{\theta}_\alpha,\, \ddot{w}_{o\alpha}\}$ is the acceleration vector. The stiffness matrix $\mathbf{K}^{st}$, geometry stiffness matrix $\mathbf{K}^{g}$ and mass matrix $\mathbf{M}$ are given as follows:

$$\mathbf{K}^{st} = \begin{pmatrix} 0.5A_{\alpha\beta\gamma\delta}\left(\partial_{,\delta\beta}\delta_{\alpha\gamma} + \partial_{,\gamma\beta}\delta_{\alpha\delta}\right) & 0.5B_{\alpha\beta\gamma\delta}\left(\partial_{,\delta\beta}\delta_{\alpha\gamma} + \partial_{,\gamma\beta}\delta_{\alpha\delta}\right) & 0 \\ 0.5B_{\alpha\beta\gamma\delta}\left(\partial_{,\delta\beta}\delta_{\alpha\gamma} + \partial_{,\gamma\beta}\delta_{\alpha\delta}\right) & 0.5D_{\alpha\beta\gamma\delta}\left(\partial_{,\delta\beta}\delta_{\alpha\gamma} + \partial_{,\gamma\beta}\delta_{\alpha\delta}\right) - H_{\alpha\beta} & -H_{\alpha\beta}\partial_{,\alpha} \\ 0 & H_{\alpha\beta}\partial_{,\alpha} & H_{\alpha\beta}\partial_{,\alpha\alpha} \end{pmatrix} \tag{20}$$

$$\mathbf{K}^{g} = \begin{pmatrix} 0 & 0 & 0 \\ 0 & 0 & 0 \\ 0 & 0 & \hat{N}_{\alpha\beta}\partial_{,\alpha\beta} \end{pmatrix}, \mathbf{M} = \begin{pmatrix} I_0 & I_1 & 0 \\ I_1 & I_2 & 0 \\ 0 & 0 & I_0 \end{pmatrix} \tag{21}$$

2.4 Analytical solution for simply-supported FG sandwich plates

The Navier solution procedure is used to obtain the analytical solutions for simply-supported boundary conditions. For this purpose, the displacement functions are expressed as product of undetermined coefficients and known trigonometric functions to satisfy the governing equations and boundary conditions. Consider a rectangular FG sandwich plate with in-plane lengths, a and b in the $x-$ and $y-$ directions, respectively (Figure 1). The Cartesian reference coordinates (x, y, z), and displacement components $(u_o,\, v_o,\, w_o)$=$(u_{o1},\, u_{o2},\, w_o)$ are used. For a simply-supported rectangular plate, the boundary conditions are given by:

$$
\begin{aligned}
&u_o(x,0,t)=0,\ \theta_x(x,0,t)=0,\ u_o(x,b,t)=0,\ \theta_x(x,b,t)=0\\
&v_o(0,y,t)=0,\ \theta_y(0,y,t)=0,\ v_o(a,y,t)=0,\ \theta_y(a,y,t)=0\\
&w_o(0,y,t)=0,\ w_o(a,y,t)=0,\ w_o(x,0,t)=0,\ w_o(x,b,t)=0\\
&N_{xx}(0,y,t)=0,\ N_{xx}(a,y,t)=0,\ N_{yy}(x,0,t)=0,\ N_{yy}(x,b,t)=0\\
&M_{xx}(0,y,t)=0,\ M_{xx}(a,y,t)=0,\ M_{yy}(x,0,t)=0,\ M_{yy}(x,b,t)=0
\end{aligned}
\tag{22}
$$

These boundary conditions allow to approximate the rotational and transverse displacements as following expansions:

$$u_o(x,y,t)=\sum_{r=1}^{\infty}\sum_{s=1}^{\infty}u_{rs}^0\cos\lambda x\,\sin\mu y\,e^{i\omega t} \tag{23}$$

$$v_o(x,y,t)=\sum_{r=1}^{\infty}\sum_{s=1}^{\infty}v_{rs}^0\sin\lambda x\,\cos\mu y\,e^{i\omega t} \tag{24}$$

$$w_o(x,y,t)=\sum_{r=1}^{\infty}\sum_{s=1}^{\infty}w_{rs}^0\sin\lambda x\,\sin\mu y\,e^{i\omega t} \tag{25}$$

$$\theta_x(x,y,t)=\sum_{r=1}^{\infty}\sum_{s=1}^{\infty}x_{rs}^0\cos\lambda x\sin\mu y\,e^{i\omega t} \tag{26}$$

$$\theta_y(x,y,t)=\sum_{r=1}^{\infty}\sum_{s=1}^{\infty}y_{rs}^0\sin\lambda x\cos\mu y\,e^{i\omega t} \tag{27}$$

where $\lambda=r\pi/a$, $\mu=s\pi/b$, ω is natural frequency of the plate, $\sqrt{i}=-1$ the imaginary unit.

Assuming that the plate is subjected to in-plane loads of form: $\hat{N}_{xx}=R_1N_0$, $\hat{N}_{yy}=R_2N_0$ (here R_1, R_2 are non-dimensional load parameters), $\hat{N}_{xy}=0$. By substituting Eqs. (23)-(27) into Eq. (19) and collecting the displacements and acceleration for any values of r and s so that $\mathbf{U}_{rs}^T=\{u_{rs}^0,v_{rs}^0,w_{rs}^0,x_{rs}^0,y_{rs}^0\}$, the following eigenvalue problem is obtained:

$$\left[\left(\mathbf{K}^{st}+\mathbf{K}^{g}\right)-\omega^2\mathbf{M}\right]\,\mathbf{U}_{rs}=0 \tag{28}$$

where the stiffness matrix $\mathbf{K}^{st}$, geometry stiffness matrix $\mathbf{K}^{g}$ and mass matrix $\mathbf{M}$ associated with the vector $\mathbf{U}_{rs}$ are expressed by:

$$\mathbf{K}^{st}=\begin{pmatrix}k_{11}&k_{12}&0&k_{14}&k_{15}\\k_{12}&k_{22}&0&k_{24}&k_{25}\\0&0&k_{33}&k_{34}&k_{35}\\k_{14}&k_{24}&k_{34}&k_{44}&k_{45}\\k_{15}&k_{25}&k_{35}&k_{45}&k_{55}\end{pmatrix},\ \mathbf{M}=\begin{pmatrix}I_0&0&0&I_1&0\\0&I_0&0&0&I_1\\0&0&I_0&0&0\\I_1&0&0&I_2&0\\0&I_1&0&0&I_2\end{pmatrix} \tag{29}$$

$$K_{ij}^g=0\quad(i,j=1,2,...,5)\quad\text{except}\quad K_{33}^g=(R_1\lambda^2+R_2\mu^2)N_0 \tag{30}$$

where,

$$
\begin{aligned}
&k_{11} = A_{1111}\lambda^2 + A_{1212}\mu^2,\ k_{12} = (A_{1122} + A_{1212})\lambda\mu,\\
&k_{14} = B_{1111}\lambda^2 + B_{1212}\mu^2, k_{15} = (B_{1122} + B_{1212})\lambda\mu,\\
&k_{22} = A_{1212}\lambda^2 + A_{2222}\mu^2,\ k_{24} = k_{15},\\
&k_{25} = B_{1212}\lambda^2 + B_{2222}\mu^2,\ k_{33} = H(\lambda^2 + \mu^2),\\
&k_{34} = H\lambda,\ k_{35} = H\mu,\ k_{44} = H + D_{1111}\lambda^2 + D_{1212}\mu^2,\\
&k_{45} = (D_{1122} + D_{1212})\lambda\mu,\ k_{55} = H + D_{2222}\mu^2 + D_{1212}\lambda^2
\end{aligned}
\tag{31}
$$

2.4.1 Buckling of FG sandwich plates

For buckling analysis, by neglecting mass matrix $\mathbf{M}$, the stability problem can be simplified as the following eigenvalue one:

$$\left(\mathbf{K}^{st} + \mathbf{K}^{g}\right)\mathbf{U}_{rs} = \mathbf{0} \tag{32}$$

To obtain a non-trivial solution, the determinant of the matrix $\mathbf{K}^{st} + \mathbf{K}^{g}$ is set equal to zero, from which the critical buckling loads (N_{cr}) of FG sandwich plates can be derived.

2.4.2 Free vibration of FG sandwich plates

For vibration under in-plane loads, the following eigenvalue problem is obtained:

$$\left(\mathbf{K}^{st} + \mathbf{K}^{g} - \omega^2\mathbf{M}\right)\mathbf{U}_{rs} = \mathbf{0} \tag{33}$$

To obtain the nontrivial solution, the determinant should be zero, i.e. $|K^{st}_{ij} + K^{g}_{ij} - \omega^2 M_{ij}| = 0$. By solving the achieved equation, the values of natural frequencies, mode shapes and load-frequency curves of simply-supported FG sandwich plates can be derived.

3 Numerical results and discussion

In this section, a number of numerical examples are analyzed for verification the accuracy of present study and investigation of the natural frequencies, critical buckling loads and load-frequency curves of simply-supported FG sandwich plates. Unless mentioned otherwise, FG sandwich plates with $b/h = 10$ made of three sets of material combinations of metal and ceramic: Al/Al_2O_3, Al/SiC, and Al/WC are considered. Their material properties are given in Table 1 and corresponding shear correction factors are shown in Table 2. Two cases of FG sandwich plates are studied:

- Hardcore: homogeneous core with Al_2O_3 or SiC or WC (E_b, ν_b, ρ_b) and FG faces with top and bottom surfaces made of Al (E_t, ν_t, ρ_t)

- Softcore: homogeneous core with Al (E_b, ν_b, ρ_b) and FG faces with top and bottom surfaces made of Al_2O_3 or SiC or WC (E_t, ν_t, ρ_t)

For convenience, the following non-dimensional critical buckling loads, natural frequencies and the relative error (%) are used:

$$\bar{N}_{cr} = \frac{N_{cr}a^2}{100E_o h^3}, \quad \mathrm{E}_o = 1\,\mathrm{GPa} \tag{34}$$

$$\bar{\omega} = \frac{\omega a^2}{h}\sqrt{\frac{\rho_o}{E_o}}, \quad \rho_o = 1\,\mathrm{kg/m^3} \tag{35}$$

$$\mathrm{Error}\,(\%) = \frac{P_c - P_m}{P_m} \times 100\% \tag{36}$$

where P_c, P_m are the results obtained from the present model and from the 5/6 shear correction factor model, respectively.

3.1 Verification studies

For verification purpose, the natural frequencies and critical buckling loads of Al/Al_2O_3 sandwich plates with homogeneous hardcore are calculated. Three different types of in-plane loads: uniaxial compression (R_1=-1, R_2=0), biaxial compressions (R_1=-1, R_2=-0.5) and (R_1=-1, R_2=-1) are considered for buckling analysis. Comparisons are given in Tables 3 and 4 on the basis of the symmetric (1-2-1) and non-symmetric (2-2-1) types of sandwich plates. The natural frequencies increase as the mode number increases while the critical buckling loads decrease with increasing aspect ratio (b/a) and R_2. It can be seen that the present approach using $\kappa = 5/6$ almost gives the identical results as Zenkour[28] based on FSDT. Besides, a good agreement between present solution and those obtained by the HSDT[28] particularly at the higher modes of vibration can be observed and discrepancy between them is also considerable.

To demonstrate the accuracy and validity of the present study further, Tables 5-8 provide fundamental natural frequencies and critical buckling loads of six types of square Al/Al_2O_3 sandwich plates with homogeneous hardcore and softcore for different values of the power-law index p. The present method is again in close agreement with the FSDT and HSDT model in Meiche et al.[30], while minor differences are shown for the comparison with the 3D solution in Li et al.[29].

3.2 Parameter studies

Parameter studies are carried out to investigate the effects of the improved shear stiffness on the natural frequencies, critical buckling loads and load-frequency curves. The (1-2-1) Al/Al_2O_3, Al/SiC, and Al/WC sandwich plates with homogeneous hardcore and softcore are considered. Figures 3 and 4 show the first three natural frequencies and critical buckling loads of Al/Al_2O_3 sandwich plate versus the power-law index under different types of loadings. Some major deviations are observed between the results of present model and that with $\kappa = 5/6$, which implies that the effect of improved shear stiffness becomes important and can not be neglected, especially for sandwich plate with homogeneous softcore. The critical buckling loads are the highest when (R_1=-1, R_2=1) and are the lowest when (R_1=-1, R_2=-1) for a specified side-to-thickness ratio. Effects of the side-to-thickness ratio and power-law index on the fundamental frequency and critical buckling load of FG sandwich plate are plotted in Figures 5 and 6. Three groups of curves are seen, for vibration analysis, the highest group is for Al/SiC sandwich plate and the lowest group is for to Al/WC one, however, for buckling analysis, the highest group is for Al/WC one and the lowest group is for to Al/Al_2O_3, respectively. The effects of the power-law index and aspect ratio on the natural frequencies and critical buckling loads of sandwich plates are also summarized in Tables 6 - 14. It can be seen that with the increase of the power-law index, the natural frequencies and critical buckling loads decrease for sandwich plate with homogeneous hardcore, and increase for sandwich plate with homogeneous softcore. This is due to the fact that higher values of power-law index correspond to high portion of metal in comparison with the ceramic part for homogeneous hardcore and inversely for homogeneous softcore. With the increase of the aspect ratio leads not only the decrease of the critical buckling loads, but also causes the changes in corresponding mode shapes. For instance, for the square plate under biaxial compression and tension ($R_1 = -1$, $R_2 = 1$), the critical buckling load occurs at $(r, s) = (2, 1)$. Since there is no reported work for the vibration and buckling of Al/Al_2O_3, Al/SiC, and Al/WC sandwich plates with homogeneous hardcore and softcore in a unitary manner as far as the authors know, it is believed that the tabulated results will be a reference with which other researchers can compare their results.

The next example is the same as before except that in this case, the effect of in-plane loads on the fundamental natural frequency is investigated. The lowest load-frequency curves of (1-2-1) rectangular FG sandwich plates with the power-law index $p = 10$ are plotted in Figures 7 and 8. All natural frequencies diminish as in-plane loads change from tension to compression, which implies that the tension loads have a stiffening effect while the compressive loads have a softening effect. The fundamental natural frequencies are the smallest for Al/WC sandwich plates and the largest for Al/SiC ones. However, as the in-plane loads increase, they decrease and interaction curve (Al/WC) intersects

two other curves (Al/Al_2O_3) and (Al/SiC) at ($\bar{N}_0$=2.2521, $\bar{\omega}$=2.0167) and ($\bar{N}_0$=2.6857, $\bar{\omega}$=1.8138), respectively, for homogeneous softcore (Figure 8b), thus, after these values, this order is changed. Finally, they vanish at 3.0961, 3.3106 and 4.5244, which correspond to the critical buckling loads of Al/Al_2O_3, Al/SiC and Al/WC sandwich plates with homogeneous softcore, respectively. Figures 7 and 8 also explain the duality between critical buckling load and fundamental natural frequency, which is the characteristic of load-frequency curves.

In order to investigate the effect of improved shear stiffness on vibration and buckling analysis further, Figures 9-12 display the relative error of the natural frequencies and critical buckling loads of FG sandwich plates with homogeneous softcore with respect to the thickness ratio of layer (e_c/e_f here $e_{ft} = e_{ft} = e_f$), power-law index p and side-to-thickness ratio (b/h). It is from these figures that confirms the effect of improved shear stiffness is more pronounced in buckling analysis than vibration one. It appears that with a specified material contrast, the maximum relative error can be found for thickness ratio of layer $e_c/e_f = 2$ corresponding to 1-2-1 FG sandwich plates (Figure 9). For such plates, with the increase of the material contrast and power-law index, the improved shear stiffness decreases, thus, the relative error increases. This error for critical buckling loads is much higher than natural frequencies. Indeed, for $p = 20$, with SiC/Al sandwich plate, the relative differences are -5.52% for the fundamental frequency and -11.01% for the critical buckling load, while with WC/Al one, these deviations are -9.82% and -19.26%, respectively (Figure 10). Relative error with respect to the power-law index for the first three natural frequencies is also plotted in Figure 11. The diagram shows that the relative error becomes more important for higher modes. Finally, effect of side-to-thickness ratio on the natural frequencies and critical buckling loads is plotted in Figure 12. It is evident from this figure that the improved shear stiffness is very effective in a relatively large region up to the point where this ratio reaches value of $b/h = 30$, which confirms again that the present improved shear stiffness should be taken into account in analysis of FG sandwich plates.

4 Conclusions

Vibration and buckling analysis of FG sandwich plates with homogeneous hardcore and softcore based on the first-order shear deformation theory have been investigated in this paper. The material property is assumed to be isotropic at each point and vary through the plate thickness according to a power-law. The improved shear stiffness and associated shear correction factors are presented. The effects of the power-law index, thickness ratio of layer, aspect ratio and material contrast on the shear correction factor, critical buckling load, natural frequency and load-frequency curves of simply-supported FG

sandwich plates are investigated. The numerical results indicate that the shear correction factor is not the same as the one of the homogeneous sandwich plate, it is a function of the power-law index, material contrast. Consequently, that leads to the differences of the fundamental natural frequency and critical buckling load between the present model and others using the five-sixth shear factor. This deviation is significant for FG sandwich plates with softcore, especially for high material contrast while this effect can be neglected for FG sandwich plate with hardcore.

Acknowledgements

The first author gratefully acknowledges financial support from Vietnam National Foundation for Science and Technology Development (NAFOSTED) under grant number 107.02-2012.07. The second author gratefully acknowledges research support fund for UoA16 from Northumbria University.

References

1 Zenkert D. The Handbook of Sandwich Construction. North European Engineering and Science Conference Series. Engineering Materials Advisory Chameleon Press Ltd, London, UK; 1997.

2 Vinson JR. The Behavior of Sandwich Structures of Isotropic and Composite Materials. Technomic Publishing Co. Inc, Lancaster, USA; 1999.

3 Feldman E, Aboudi J. Buckling analysis of functionally graded plates subjected to uniaxial loading. Composite Structures. 1997;38:29–36.

4 Javaheri R, Eslami MR. Buckling of functionally graded plates under in-plane compressive loading. Journal of Applied Mathematics and Mechanics. 2002;82:277–283.

5 Mahdavian M. Buckling analysis of simply-supported functionally graded rectangular plates under non-uniform in-plane compressive loading. Journal of Solid Mechanics. 2009;1:213–225.

6 Mohammadi M, Saidi AR, Jomehzadeh E. Levy solution for buckling analysis of functionally graded rectangular plates. Applied Composite Materials. 2010;17:81–93.

7 Chen CS, Chen TJ, Chien RD. Nonlinear vibration of initially stressed functionally graded plates. Thin-Walled Structures. 2006;44(8):844–851.

8 Baferani AH, Saidi AR, Jomehzadeh E. An exact solution for free vibration of thin functionally

graded rectangular plates. Proceedings of the Institution of Mechanical Engineers, Part C: Journal of Mechanical Engineering Science. 2011;225:526–536.

9 Zhao X, Lee YY, Liew KM. Mechanical and thermal buckling analysis of functionally graded plates. Composite Structures. 2009;90:161–171.

10 Zhao X, Lee YY, Liew KM. Free vibration analysis of functionally graded plates using the element-free kp-Ritz method. Journal of Sound and Vibration. 2009;319:918–939.

11 Mokhtar B, Abedlouahed T, Abbas ABE, Abdelkader M. Buckling analysis of functionally graded plates with simply supported edges. Leonardo Journal of Sciences. 2009;8:21–32.

12 Hosseini-Hashemi S, Taher HRD, Akhavan H, Omidi M. Free vibration of functionally graded rectangular plates using first-order shear deformation plate theory. Applied Mathematical Modelling. 2010;34:1276–1291.

13 Hosseini-Hashemi S, Fadaee M, Atashipour SR. A new exact analytical approach for free vibration of Reissner-Mindlin functionally graded rectangular plates. International Journal of Mechanical Sciences. 2011;53:11–22.

14 Mohammadi M, Saidi AR, Jomehzadeh E. A novel analytical approach for the buckling analysis of moderately thick functionally graded rectangular plates with two simply-supported opposite edges. Proceedings of the Institution of Mechanical Engineers, Part C: Journal of Mechanical Engineering Science. 2010;224:1831–1841.

15 Reddy JN. Analysis of functionally graded plates. International Journal for Numerical Methods in Engineering. 2000;47:663–684.

16 Zenkour AM. Generalized shear deformation theory for bending analysis of functionally graded materials. Applied Mathematical Modelling. 2006;30:67–84.

17 Pradyumna S, Bandyopadhyay JN. Free vibration analysis of functionally graded curved panels using a higher-order finite element formulation. Journal of Sound and Vibration. 2008;318:176–192.

18 Matsunaga H. Free vibration and stability of functionally graded plates according to a 2-D higher-order deformation theory. Composite Structures. 2008;82:499–512.

19 Chen CS, Hsu CY, Tzou GJ. Vibration and stability of functionally graded plates based on a higher-order deformation theory. Journal of Reinforced Plastics and Composites. 2009;28:1215–1234.

20 Talha M, Singh BN. Static response and free vibration analysis of FGM plates using higher order shear deformation theory. Applied Mathematical Modelling. 2010;34:3991–4011.

21 Reddy JN. A general nonlinear third-order theory of functionally graded plates. International Journal of Aerospace and Lightweight Structures. 2011;1:1–21.

22 Neves AMA, Ferreira AJM, Carrera E, Cinefra M, Roque CMC, Jorge RMN. A quasi-3D hyperbolic shear deformation theory for the static and free vibration analysis of functionally graded plates. Composite Structures. 2012;94:1814–1825.

23 Mantari JL, Soares CG. A novel higher-order shear deformation theory with stretching effect for functionally graded plates. Composites Part B: Engineering. 2013;45(1):268 – 281.

24 Jha DK, Kant T, Singh RK. Free vibration response of functionally graded thick plates with shear and normal deformations effects. Composite Structures. 2013;96:799–823.

25 Thai HT, Vo TP. A new sinusoidal shear deformation theory for bending, buckling, and vibration of functionally graded plates. Applied Mathematical Modelling. 2013; 37: 3269 – 3281

26 Thai HT, Kim SE. A simple quasi-3D sinusoidal shear deformation theory for functionally graded plates. Composite Structures. 2013;99(0):172 – 180.

27 Thai HT, Vo TP, Bui TQ, Nguyen TK. A quasi-3D hyperbolic shear deformation theory for functionally graded plates. Acta Mechanica. 2013, In Press.

28 Zenkour AM. A comprehensive analysis of functionally graded sandwich plates: Part 2 - Buckling and free vibration. International Journal of Solids and Structures. 2005;42:5243–5258.

29 Li Q, Iu VP, Kou KP. Three-dimensional vibration analysis of functionally graded material sandwich plates. Journal of Sound and Vibration. 2008;311:498–515.

30 Meiche NE, Tounsi A, Ziane N, Mechab I, Bedia EAA. A new hyperbolic shear deformation theory for buckling and vibration of functionally graded sandwich plate. International Journal of Mechanical Sciences. 2011;53(4):237 – 247.

31 Bourada M, Tounsi A, Houari MSA, Bedia EAA. A new four-variable refined plate theory for thermal buckling analysis of functionally graded sandwich plates. Journal of Sandwich Structures and Materials. 2011;14:5–33.

32 Xiang S, Jin Y, Bi Z, Jiang S, Yang MS. A n-order shear deformation theory for free vibration of functionally graded and composite sandwich plates. Composite Structures. 2011;93:2826–2832.

33 Natarajan S, Manickam G. Bending and vibration of functionally graded material sandwich plates using an accurate theory. Finite Elements in Analysis and Design. 2012;57:32 – 42.

34 Neves AMA, Ferreira AJM, Carrera E, Cinefra M, Roque CMC, Jorge RMN. Static, free vibration and buckling analysis of isotropic and sandwich functionally graded plates using a quasi-3D higher-order shear deformation theory and a meshless technique. Composites Part B: Engineering. 2013;44:657–674.

35 Nguyen TK, Sab K, Bonnet G. First-order shear deformation plate models for functionally graded materials. Composite Structures. 2008;83:25–36.

36 Nguyen TK, Vo TP, Thai HT. Static and free vibration of axially loaded functionally graded beams based on the first-order shear deformation theory. Composites Part B: Engineering. 2013;55:147–157.

37 Hill R. The elastic behavior of a crystalline aggregate. Proceeding of the Physical Society. 1952;65:349–354.

38 Rolfes R, Rohwer K. Improved transverse shear stresses in composite finite elements based on first order shear deformation theory. International Journal for Numerical Methods in Engineering. 1997;40:51–60.

39 Berthelot JM. Composite Materials: Mechanical Behavior and Structural Analysis. New York: Springer; 1999.

40 Vlachoutsis S. Shear correction factors for plates and shells. International Journal for Numerical Methods in Engineering. 1992;33:1537–1552.

CAPTIONS OF FIGURES

Figure 1: Geometry of a functionally graded three-layer sandwich plate.

Figure 2: Distribution of material through the plate thickness according to the power-law form.

Figure 3: Effect of the power-law index p on the first three natural frequencies of (1-2-1) square Al/Al_2O_3 sandwich plate.

Figure 4: Effect of the power-law index p on non-dimensional critical buckling loads ($\bar{N}_{cr}$) of (1-2-1) square Al/Al_2O_3 sandwich plate under different loading conditions.

Figure 5: A 3D diagram of the power-law index p, side-to-thickness ratio (b/h) and nondimensional fundamental natural frequency of (1-2-1) square FG sandwich plate.

Figure 6: A 3D diagram of the power-law index p, side-to-thickness ratio (b/h) and nondimensional critical buckling load of (1-2-1) square FG sandwich plate ($R_1 = -1$, $R_2 = 0$).

Figure 7: Effect of in-plane loads on the nondimensional fundamental frequency of (1-2-1) rectangular Al/Al_2O_3 sandwich plates ($b/a = 2$, $p = 10$) with homogeneous hardcore and softcore.

Figure 8: Effect of in-plane loads on the nondimensional fundamental frequency of (1-2-1) rectangular FG sandwich plates ($b/a = 2$, $p = 10$) with homogeneous hardcore and softcore ($R_1 = -1$, $R_2 = 0$).

Figure 9: Relative error (%) of the critical buckling loads ($R_1 = -1$, $R_2 = 0$) and fundamental frequencies of square FG sandwich plates with homogeneous softcore with respect to the thickness ratio of layer e_c/e_f ($p = 10$).

Figure 10: Relative error (%) of the critical buckling loads ($R_1 = -1$, $R_2 = 0$) and fundamental frequencies of (1-2-1) square FG sandwich plates with homogeneous softcore with respect to the power-law index p.

Figure 11: Relative error (%) of the first three natural frequencies of (1-2-1) square sandwich plate with homogeneous softcore with respect to the power-law index p.

Figure 12: Relative error (%) of the critical buckling loads ($R_1 = -1$, $R_2 = 0$) and fundamental frequencies of (1-2-1) square FG sandwich plates with homogeneous softcore with respect to the side-to-thickness ratio (b/h) ($p = 10$).

CAPTIONS OF TABLES

Table 1: Material properties of metal and ceramic.

Table 2: Effect of the power-law index p and thickness ratio of layer on shear correction factors for various FG sandwich plates with homogeneous hardcore and softcore.

Table 3: Nondimensional natural frequencies ($\bar{\omega}$) of Al/Al_2O_3 sandwich plates with homogeneous hardcore ($p = 2$).

Table 4: Nondimensional critical buckling loads ($\bar{N}_{cr}$) of Al/Al_2O_3 sandwich plates with homogeneous hardcore ($p = 2$).

Table 5: Nondimensional fundamental frequency ($\bar{\omega}$) of square Al/Al_2O_3 sandwich plates with homogeneous hardcore and softcore.

Table 6: Nondimensional critical buckling loads ($\bar{N}_{cr}$) of square Al/Al_2O_3 sandwich plates subjected to uniaxial compressive load ($R_1 = -1, R_2 = 0$) with homogeneous hardcore and softcore.

Table 7: Nondimensional critical buckling load ($\bar{N}_{cr}$) of square Al/Al_2O_3 sandwich plates subjected to biaxial compressive loads ($R_1 = -1, R_2 = -1$) with homogeneous hardcore and softcore.

Table 8: Nondimensional critical buckling loads ($\bar{N}_{cr}$) of square Al/Al_2O_3 sandwich plates subjected to axial compression and tension ($R_1 = -1, R_2 = 1$) with homogeneous hardcore and softcore ($r = 2, s = 1$).

Table 9: The first three non-dimensional natural frequencies ($\bar{\omega}$) of (1-2-1) Al/Al_2O_3 sandwich plates with homogeneous hardcore and softcore.

Table 10: Nondimensional critical buckling loads ($\bar{N}_{cr}$) of (1-2-1) Al/Al_2O_3 sandwich plates with homogeneous hardcore and softcore.

Table 11: The first three non-dimensional natural frequencies ($\bar{\omega}$) of (1-2-1) Al/SiC sandwich plates with homogeneous hardcore and softcore.

Table 12: Nondimensional critical buckling load ($\bar{N}_{cr}$) of (1-2-1) Al/SiC sandwich plates with homogeneous hardcore and softcore.

Table 13: The first three non-dimensional natural frequencies ($\bar{\omega}$) of (1-2-1) Al/WC sandwich plates with homogeneous hardcore and softcore.

Table 14: Nondimensional critical buckling load ($\bar{N}_{cr}$) of (1-2-1) Al/WC sandwich plates with homogeneous hardcore and softcore.

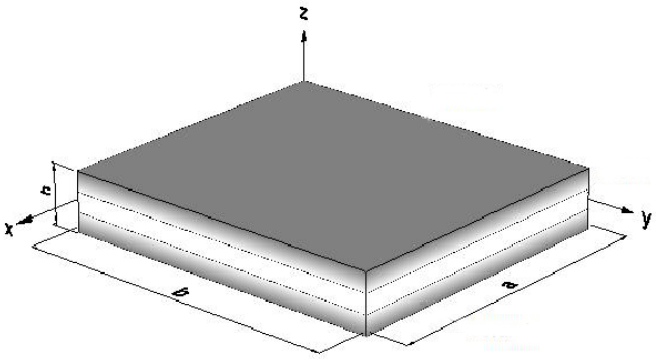

(a)

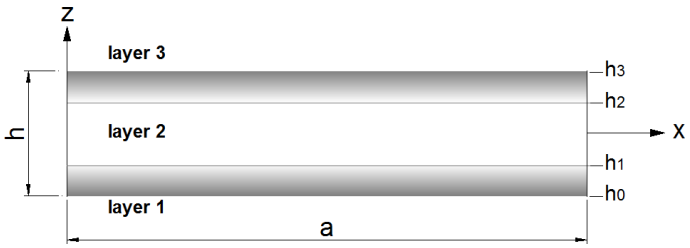

(b)

Figure 1: Geometry of a functionally graded three-layer sandwich plate.

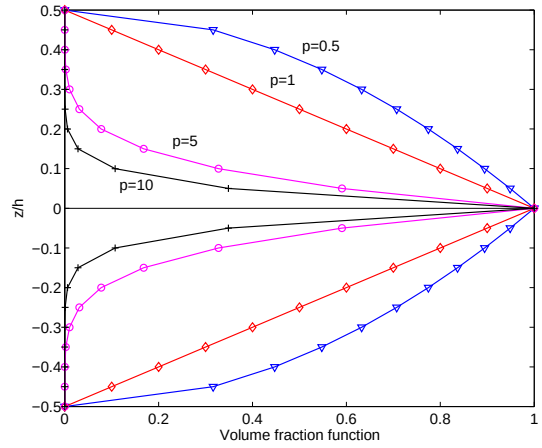

(a) 1-0-1

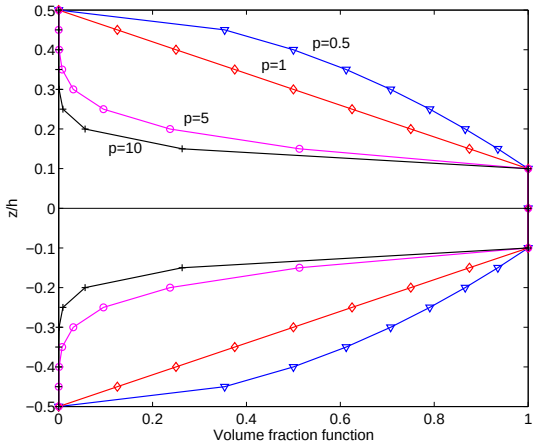

(b) 2-1-2

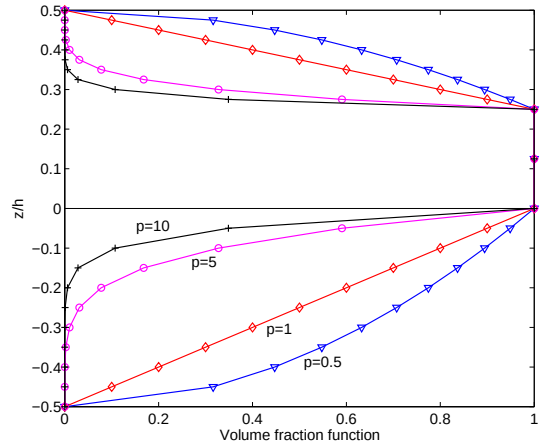

(c) 2-1-1

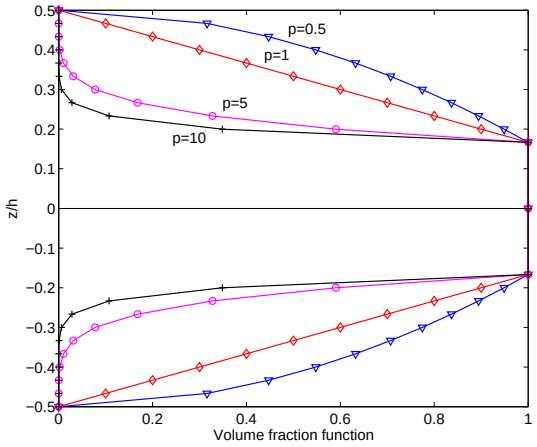

(d) 1-1-1

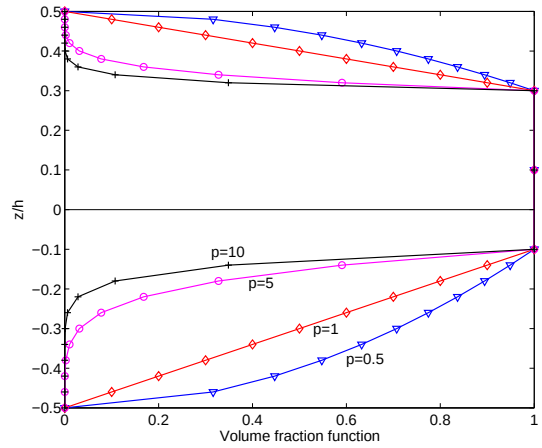

(e) 2-2-1

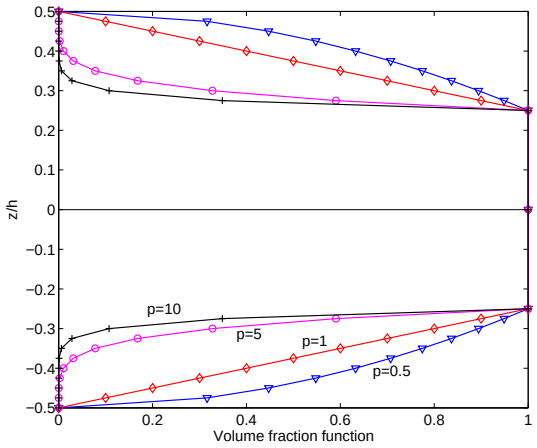

(f) 1-2-1

Figure 2: Distribution of material through the plate thickness according to the power-law form.

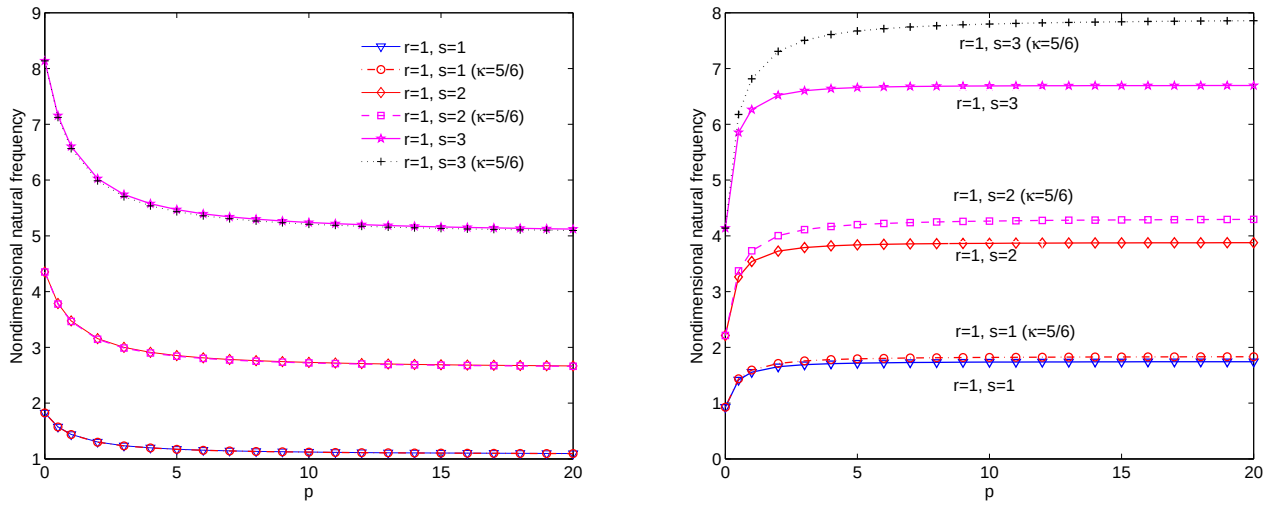

(a) Homogeneous hardcore

(b) Homogeneous softcore

Figure 3: Effect of the power-law index p on the first three natural frequencies of (1-2-1) square Al/Al_2O_3 sandwich plate.

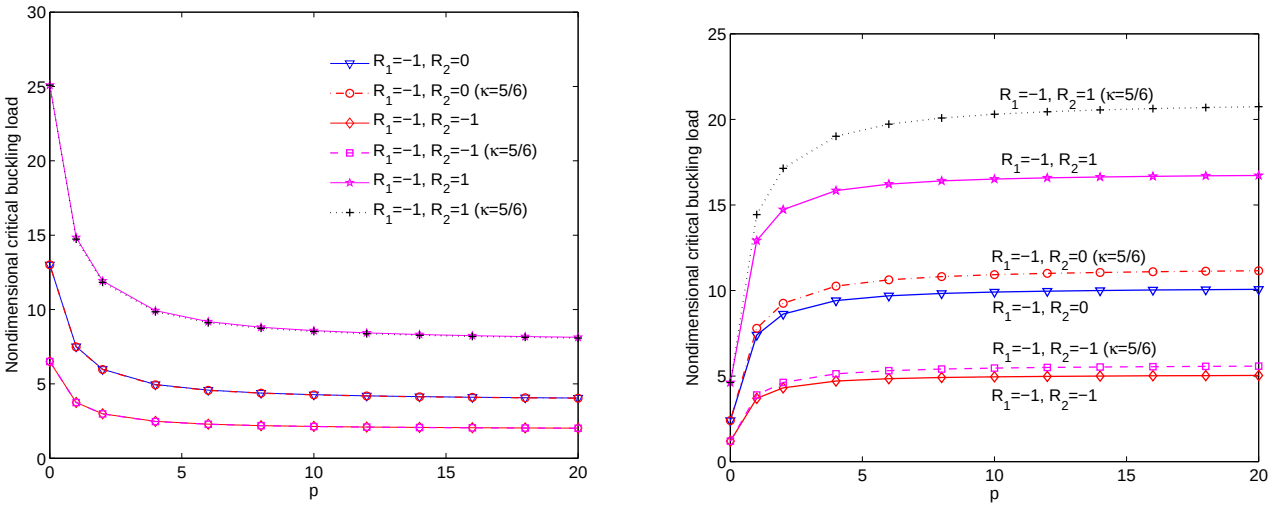

(a) Homogeneous hardcore

(b) Homogeneous softcore

Figure 4: Effect of the power-law index p on non-dimensional critical buckling loads ($\bar{N}_{cr}$) of (1-2-1) square Al/Al_2O_3 sandwich plate under different loading conditions.

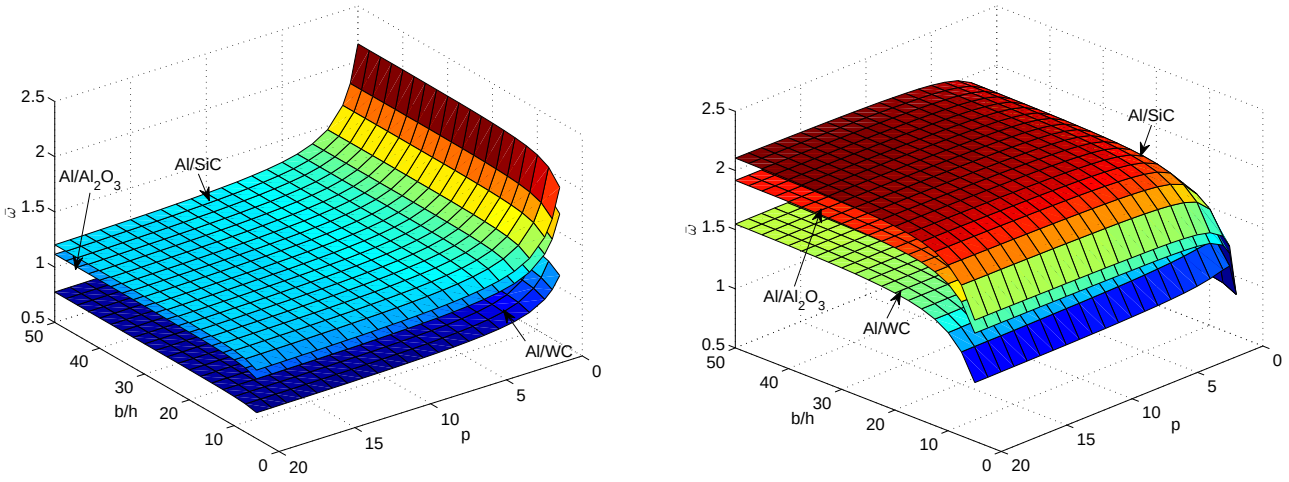

(a) Hardcore

(b) Softcore

Figure 5: A 3D diagram of the power-law index p, side-to-thickness ratio (b/h) and nondimensional fundamental natural frequency of (1-2-1) square FG sandwich plate.

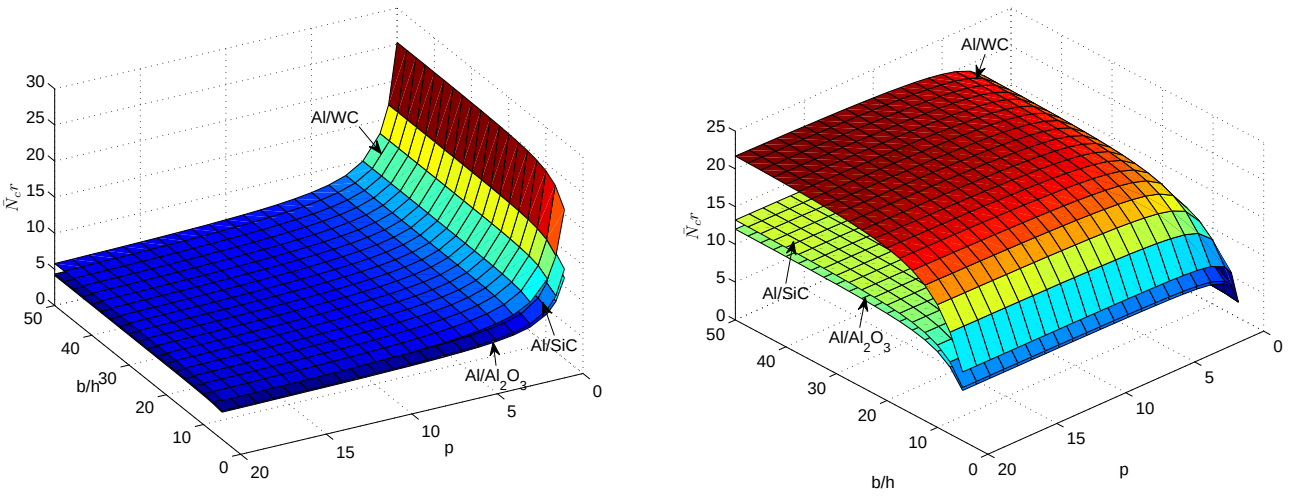

(a) Hardcore

(b) Softcore

Figure 6: A 3D diagram of the power-law index p, side-to-thickness ratio (b/h) and nondimensional critical buckling load of (1-2-1) square FG sandwich plate ($R_1 = -1$, $R_2 = 0$).

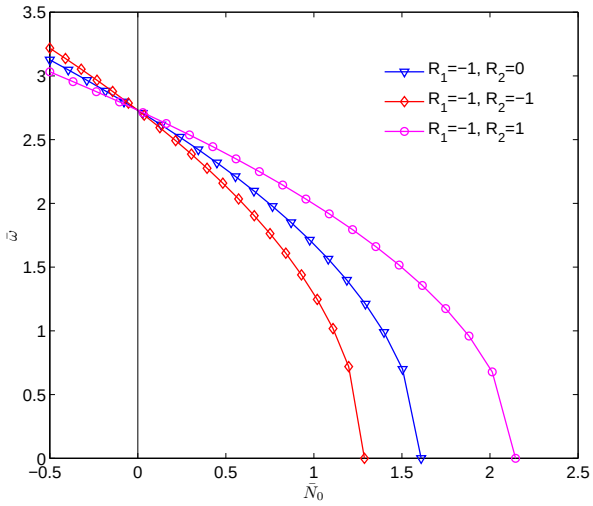

(a) Homogeneous hardcore

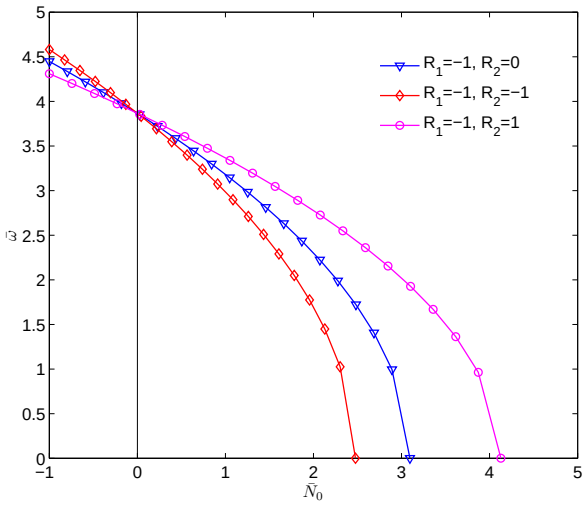

(b) Homogeneous softcore

Figure 7: Effect of in-plane loads on the nondimensional fundamental frequency of (1-2-1) rectangular Al/Al_2O_3 sandwich plates ($b/a = 2$, $p = 10$) with homogeneous hardcore and softcore.

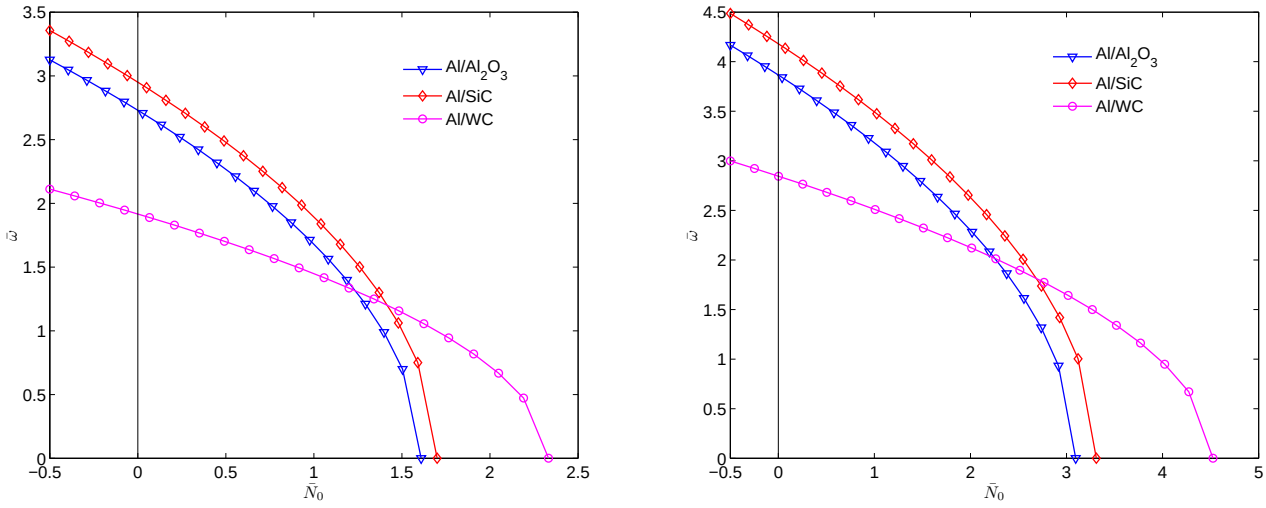

(a) Homogeneous hardcore

(b) Homogeneous softcore

Figure 8: Effect of in-plane loads on the nondimensional fundamental frequency of (1-2-1) rectangular FG sandwich plates ($b/a = 2$, $p = 10$) with homogeneous hardcore and softcore ($R_1 = -1$, $R_2 = 0$).

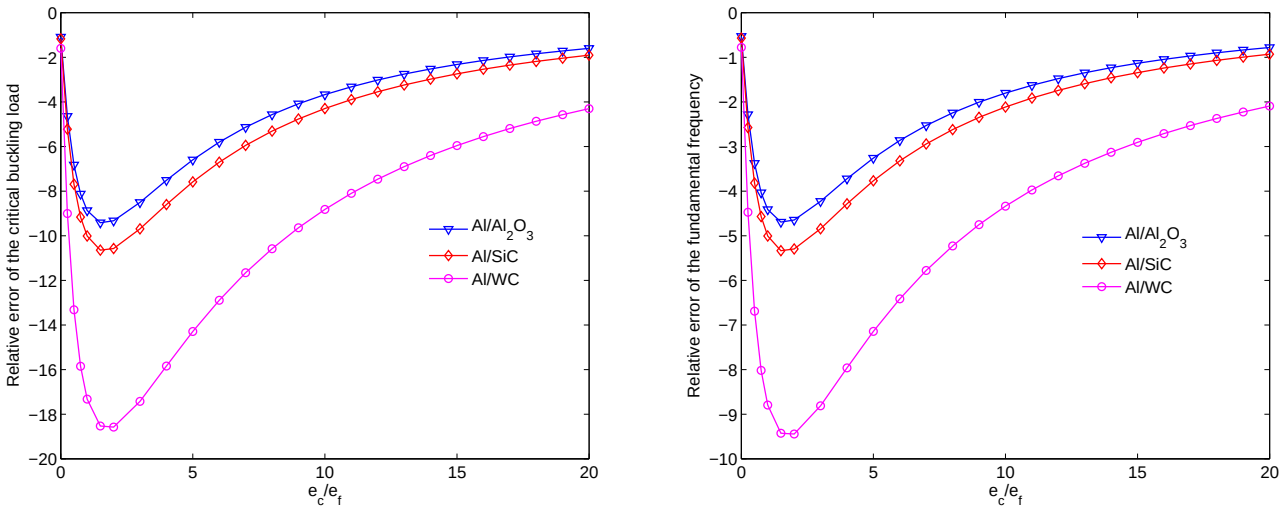

(a) Critical buckling loads

(b) Fundamental frequencies

Figure 9: Relative error (%) of the critical buckling loads ($R_1 = -1$, $R_2 = 0$) and fundamental frequencies of square FG sandwich plates with homogeneous softcore with respect to the thickness ratio of layer e_c/e_f ($p = 10$).

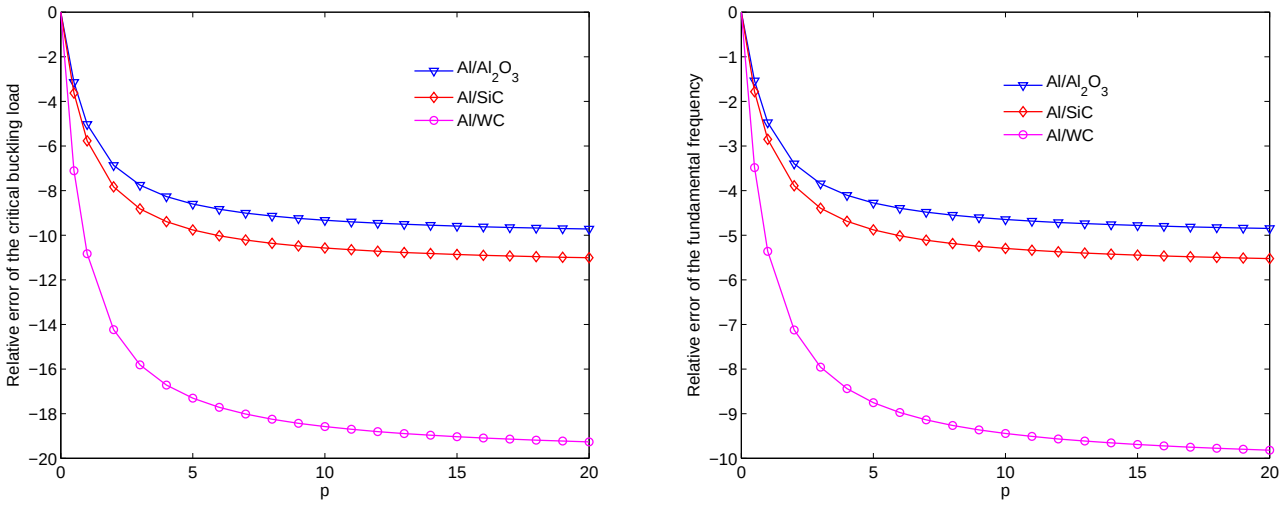

(a) Critical buckling loads

(b) Fundamental frequencies

Figure 10: Relative error (%) of the critical buckling loads ($R_1 = -1$, $R_2 = 0$) and fundamental frequencies of (1-2-1) square FG sandwich plates with homogeneous softcore with respect to the power-law index p.

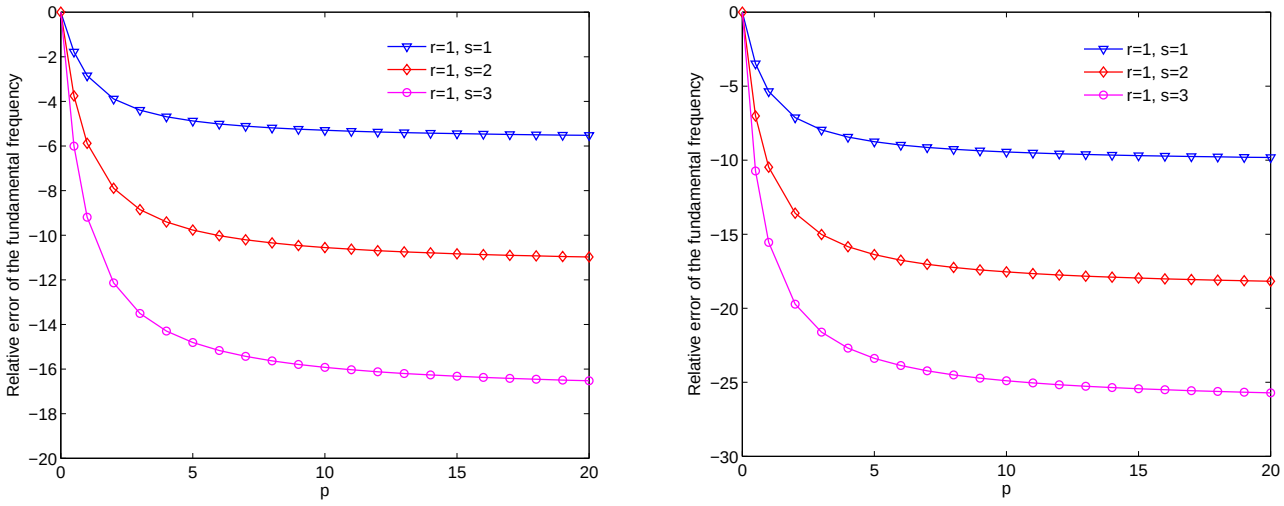

(a) Al/SiC

(b) Al/WC

Figure 11: Relative error (%) of the first three natural frequencies of (1-2-1) square sandwich plate with homogeneous softcore with respect to the power-law index p

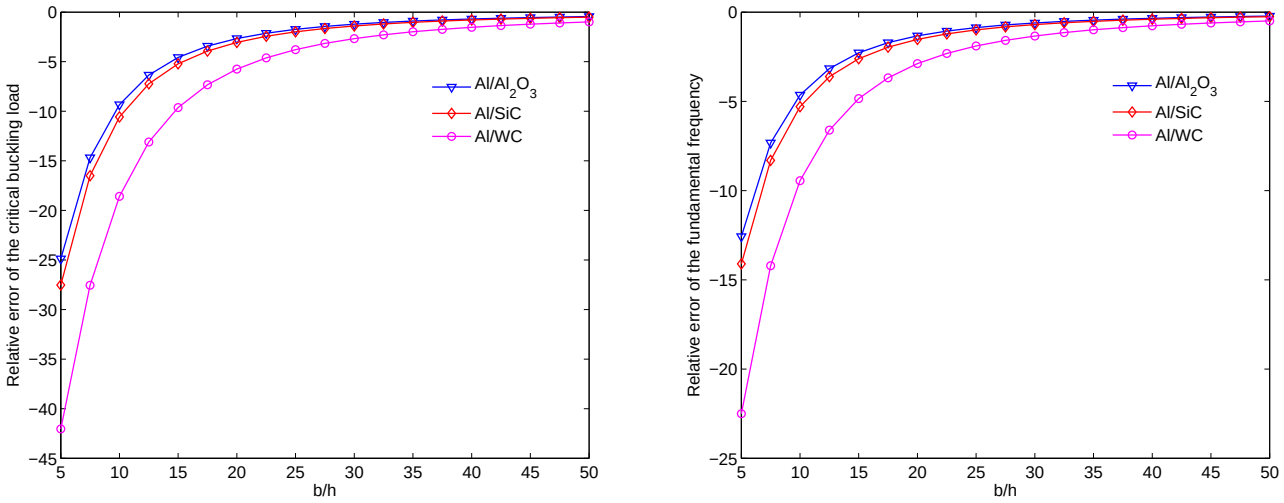

(a) Critical buckling loads

(b) Fundamental frequencies

Figure 12: Relative error (%) of the critical buckling loads ($R_1 = -1$, $R_2 = 0$) and fundamental frequencies of (1-2-1) square FG sandwich plates with homogeneous softcore with respect to the side-to-thickness ratio (b/h) ($p = 10$).

Table 1: Material properties of metal and ceramic

Material	Young's modulus (GPa)	Mass density (kg/m^3)	Poisson's ratio
Aluminum (Al)	70	2707	0.3
Alumina (Al_2O_3)	380	3800	0.3
Silicon carbide (SiC)	420	3210	0.3
Tungsten carbide (WC)	700	15800	0.3

Table 2: Effect of the power-law index p and thickness ratio of layer on shear correction factors for various FG sandwich plates with homogeneous hardcore and softcore.

Core	E_t/E_b	p	Thickness ratio of layer					
			1-0-1	2-1-2	2-1-1	1-1-1	2-2-1	1-2-1
Hardcore	7/38	0	0.8333	0.8333	0.8333	0.8333	0.8333	0.8333
		0.5	0.9105	0.9072	0.8936	0.8979	0.8861	0.8789
		1.0	0.9489	0.9473	0.9219	0.9333	0.9128	0.9016
		5.0	0.8633	0.8953	0.8261	0.9471	0.9076	0.9398
		10.0	0.8131	0.7919	0.7176	0.8793	0.8431	0.9309
	7/42	0.5	0.9130	0.9086	0.8951	0.8990	0.8869	0.8796
		1.0	0.9514	0.9494	0.9234	0.9347	0.9139	0.9021
		5.0	0.8554	0.8902	0.8198	0.9464	0.9071	0.9384
		10.0	0.8012	0.7757	0.7007	0.8720	0.8374	0.9284
	7/70	0.5	0.9188	0.9143	0.8990	0.9035	0.8903	0.8818
		1.0	0.9602	0.9561	0.9286	0.9387	0.9169	0.9029
		5.0	0.8062	0.8686	0.7982	0.9436	0.9072	0.9276
		10.0	0.7212	0.6941	0.6244	0.8404	0.8176	0.9134
Softcore	38/7	0.5	0.6048	0.5635	0.5793	0.5634	0.5835	0.5899
		1.0	0.5730	0.4929	0.5062	0.4837	0.5029	0.5071
		5.0	0.6362	0.4073	0.4134	0.3754	0.3899	0.3881
		10.0	0.6987	0.3961	0.4003	0.3570	0.3704	0.3666
	42/7	0.5	0.5881	0.5420	0.5571	0.5408	0.5610	0.5673
		1.0	0.5573	0.4698	0.4821	0.4591	0.4776	0.4819
		5.0	0.6250	0.3825	0.3873	0.3502	0.3636	0.3623
		10.0	0.6905	0.3706	0.3738	0.3317	0.3442	0.3409
	70/7	0.5	0.5079	0.4316	0.4428	0.4234	0.4410	0.4473
		1.0	0.4827	0.3573	0.3636	0.3401	0.3536	0.3574
		5.0	0.5713	0.2693	0.2694	0.2385	0.2470	0.2468
		10.0	0.6501	0.2560	0.2553	0.2218	0.2299	0.2284

Table 3: Nondimensional natural frequencies ($\bar{\omega}$) of Al/Al_2O_3 sandwich plates with homogeneous hardcore ($p = 2$).

(r, s)	$1-2-1$				$2-2-1$			
	Present	Present ($\kappa = 5/6$)	Zenkour[28] (FSDT)	Zenkour[28] (HSDT)	Present	Present ($\kappa = 5/6$)	Zenkour[28] (FSDT)	Zenkour[28] (HSDT)
(1, 1)	1.30230	1.30020	1.30020	1.30246	1.24360	1.24148	1.26524	1.26775
(1, 2)	3.15631	3.14459	3.14452	3.15698	3.01630	3.00441	3.05968	3.07353
(2, 2)	4.90792	4.88084	4.88021	4.90879	4.69323	4.66572	4.74815	4.77998
(1, 3)	6.02622	5.98651	5.98487	6.02667	5.76484	5.72448	5.82264	5.86924
(2, 3)	7.63842	7.57701	7.57215	7.63674	7.31097	7.24850	7.36640	7.43850
(1, 4)	9.68108	9.58685	9.57284	9.67233	9.27185	9.17590	9.31198	9.42315
(3, 3)	10.17464	10.07165	10.05424	10.16314	9.74595	9.64106	9.78007	9.90179
(2, 4)	11.14296	11.02194	10.99612	11.12461	10.67641	10.55310	10.69588	10.83951
(3, 4)	13.46402	13.29541	13.23801	13.41936	12.90836	12.73640	12.87543	13.07809
(4, 4)	16.50757	16.26819	16.13722	16.40035	15.83825	15.59388	15.69346	15.98701

Table 4: Nondimensional critical buckling loads ($\bar{N}_{cr}$) of Al/Al_2O_3 sandwich plates with homogeneous hardcore ($p = 2$).

(R_1, R_2)	b/a	$1-2-1$				$2-2-1$			
		Present	Present ($\kappa = 5/6$)	Zenkour[28] (FSDT)	Zenkour[28] (HSDT)	Present	Present ($\kappa = 5/6$)	Zenkour[28] (FSDT)	Zenkour[28] (HSDT)
(-1, 0)	0.5[a]	23.94086	23.86154	23.86154	23.94786	21.37497	21.29983	21.29983	21.38582
	1.0	5.98521	5.96539	5.96539	5.98697	5.34374	5.32496	5.32496	5.32496
	2.0	2.23594	2.21831	2.21831	2.23758	2.00028	1.98352	1.98352	2.00278
(-1, -0.5)	0.5	12.61310	12.58665	12.58665	12.61540	11.25535	11.23031	11.23031	11.25893
	1.0	3.99014	3.97692	3.97692	3.99131	3.56250	3.54997	3.54997	3.56430
	2.0	1.98750	1.97183	1.97183	1.98896	1.77803	1.76313	1.76313	1.78025
(-1, -1)	0.5	7.56786	7.55199	7.55199	7.56924	6.75321	6.73819	6.73819	6.75536
	1.0	2.99261	2.98269	2.98269	2.99348	2.67187	2.66248	2.66248	2.67323
	2.0	1.78875	1.77464	1.77464	1.79006	1.60022	1.58681	1.58681	1.60222

(a) : Critical buckling occurs at $(r, s) = (2, 1)$.

Table 5: Nondimensional fundamental frequency ($\bar{\omega}$) of square Al/Al_2O_3 sandwich plates with homogeneous hardcore and softcore.

Core	p	Theory	$\bar{\omega}$					
			1-0-1	2-1-2	2-1-1	1-1-1	2-2-1	1-2-1
Hardcore	0	Present	1.82442	1.82442	1.82442	1.82442	1.82442	1.82442
		Present ($\kappa = 5/6$)	1.82442	1.82442	1.82442	1.82442	1.82442	1.82442
		Meiche et al.[30] (FSDT)	1.82442	1.82442	1.82442	1.82442	1.82442	1.82442
		Meiche et al.[30] (HSDT)	1.82445	1.82445	1.82445	1.82445	1.82445	1.82445
	0.5	Present	1.44321	1.48332	1.50567	1.51862	1.54655	1.57407
		Present ($\kappa = 5/6$)	1.44075	1.48088	1.50359	1.51638	1.54462	1.57234
		Meiche et al.[30] (FSDT)	1.44168	1.48159	1.51035	1.51695	1.55001	1.57274
		Meiche et al.[30] (HSDT)	1.44424	1.48408	1.51253	1.51922	1.55199	1.57451
	1.0	Present	1.24294	1.29999	1.33320	1.35328	1.39559	1.43927
		Present ($\kappa = 5/6$)	1.24032	1.29729	1.33093	1.35072	1.39336	1.43722
		Meiche et al.[30] (FSDT)	1.24031	1.29729	1.34637	1.35072	1.40555	1.43722
		Meiche et al.[30] (HSDT)	1.24320	1.30011	1.34888	1.35333	1.40789	1.43934
	5.0	Present	0.94311	0.97960	1.02781	1.04347	1.10771	1.17348
		Present ($\kappa = 5/6$)	0.94257	0.97870	1.02793	1.04183	1.10646	1.17159
		Meiche et al.[30] (FSDT)	0.94256	0.97870	1.07156	1.04183	1.14467	1.17159
		Meiche et al.[30] (HSDT)	0.94598	0.98184	1.07432	1.04466	1.14731	1.17397
	10.0	Present	0.92464	0.93896	0.98718	0.99321	1.05866	1.12226
		Present ($\kappa = 5/6$)	0.92508	0.93961	0.98937	0.99256	1.05849	1.12067
		Meiche et al.[30] (FSDT)	0.92508	0.93962	1.03580	0.99256	1.10261	1.12067
		Meiche et al.[30] (HSDT)	0.92839	0.94297	1.03862	0.99551	1.10533	1.12314
Softcore	0	Present	0.92775	0.92775	0.92775	0.92775	0.92775	0.92775
		Present ($\kappa = 5/6$)	0.92775	0.92775	0.92775	0.92775	0.92775	0.92775
		Li et al[29] (3D)	0.92897	0.92897	-	0.92897	0.92897	0.92897
	0.5	Present	1.57103	1.52374	1.48178	1.48288	1.43262	1.41475
		Present ($\kappa = 5/6$)	1.59164	1.55034	1.50475	1.50942	1.45484	1.43687
		Li et al[29] (3D)	1.57352	1.52588	-	1.48459	1.43419	1.41662
	1.0	Present	1.71619	1.66822	1.61869	1.62652	1.56650	1.55414
		Present ($\kappa = 5/6$)	1.74266	1.71023	1.65563	1.67122	1.60446	1.59360
		Li et al[29] (3D)	1.72227	1.67437	-	1.63053	1.57037	1.55788
	5.0	Present	1.83222	1.79962	1.75239	1.77215	1.71157	1.71736
		Present ($\kappa = 5/6$)	1.84879	1.86166	1.80983	1.84927	1.77966	1.79408
		Li et al[29] (3D)	1.84198	1.82611	-	1.78956	1.72726	1.72670
	10.0	Present	1.83231	1.80483	1.76179	1.78266	1.72538	1.73573
		Present ($\kappa = 5/6$)	1.84209	1.86791	1.82121	1.86498	1.79890	1.82035
		Li et al[29] (3D)	1.84020	1.83987	-	1.80813	1.74779	1.74811

Table 6: Nondimensional critical buckling loads ($\bar{N}_{cr}$) of square Al/Al_2O_3 sandwich plates subjected to uniaxial compressive load ($R_1 = -1, R_2 = 0$) with homogeneous hardcore and softcore.

Core	p	Theory	$\bar{N}_{cr}$					
			1-0-1	2-1-2	2-1-1	1-1-1	2-2-1	1-2-1
Hardcore	0	Present	13.00449	13.00449	13.00449	13.00449	13.00449	13.00449
		Present ($\kappa = 5/6$)	13.00449	13.00449	13.00449	13.00449	13.00449	13.00449
		Meiche et al.[30] (FSDT)	13.00449	13.00449	13.00449	13.00449	13.00449	13.00449
		Meiche et al.[30] (HSDT)	13.00495	13.00495	13.00495	13.00495	13.00495	13.00495
	0.5	Present	7.35358	7.93243	8.21646	8.42959	8.80290	9.21133
		Present ($\kappa = 5/6$)	7.32784	7.90563	8.19306	8.40405	8.78033	9.19048
		Meiche et al.[30] (FSDT)	7.33732	7.91320	8.20015	8.41034	8.78673	9.19517
		Meiche et al.[30] (HSDT)	7.36437	7.94084	8.22470	8.43645	8.80997	9.21681
	1	Present	5.16478	5.83869	6.19190	6.46405	6.94849	7.50558
		Present ($\kappa = 5/6$)	5.14236	5.81379	6.17020	6.43892	6.92571	7.48365
		Meiche et al.[30] (FSDT)	5.14236	5.81379	6.17020	6.43892	6.92571	7.48365
		Meiche et al.[30] (HSDT)	5.16713	5.84006	6.19394	6.46474	6.94944	7.50656
	5	Present	2.64159	3.02825	3.38458	3.57105	4.10238	4.73046
		Present ($\kappa = 5/6$)	2.63849	3.02255	3.38542	3.55959	4.09286	4.71474
		Meiche et al.[30] (FSDT)	2.63842	3.02252	3.38538	3.55958	4.09285	4.71475
		Meiche et al.[30] (HSDT)	2.65821	3.04257	3.40351	3.57956	4.11209	4.73469
	10	Present	2.46665	2.72231	3.06028	3.17949	3.69009	4.27289
		Present ($\kappa = 5/6$)	2.46906	2.72623	3.07431	3.17520	3.68893	4.26044
		Meiche et al.[30] (FSDT)	2.46904	2.72626	3.07428	3.17521	3.68890	4.26040
		Meiche et al.[30] (HSDT)	2.48727	2.74632	3.09190	3.19471	3.70752	4.27991
Softcore	0	Present	2.39556	2.39556	2.39556	2.39556	2.39556	2.39556
		Present ($\kappa = 5/6$)	2.39556	2.39556	2.39556	2.39556	2.39556	2.39556
	0.5	Present	7.79154	7.15372	6.72642	6.66497	6.17198	5.94182
		Present ($\kappa = 5/6$)	8.00364	7.41326	6.94300	6.91286	6.37091	6.13472
	1	Present	9.84984	8.98965	8.39322	8.34645	7.65362	7.39422
		Present ($\kappa = 5/6$)	10.16533	9.46203	8.79268	8.82558	8.04067	7.78586
	5	Present	12.48575	11.42654	10.69312	10.68481	9.78827	9.57415
		Present ($\kappa = 5/6$)	12.71956	12.25225	11.42742	11.66389	10.60706	10.47513
	10	Present	12.77338	11.71323	11.00449	10.99040	10.09684	9.90637
		Present ($\kappa = 5/6$)	12.91427	12.57142	11.78218	12.06023	11.00259	10.92575

Table 7: Nondimensional critical buckling load ($\bar{N}_{cr}$) of square Al/Al_2O_3 sandwich plates subjected to biaxial compressive loads ($R_1 = -1, R_2 = -1$) with homogeneous hardcore and softcore.

Core	p	Theory	$\bar{N}_{cr}$					
			1-0-1	2-1-2	2-1-1	1-1-1	2-2-1	1-2-1
Hardcore	0	Present	6.50224	6.50224	6.50224	6.50224	6.50224	6.50224
		Present ($\kappa = 5/6$)	6.50224	6.50224	6.50224	6.50224	6.50224	6.50224
		Meiche et al.[30] (FSDT)	6.50224	6.50224	6.50224	6.50224	6.50224	6.50224
		Meiche et al.[30] (HSDT)	6.50248	6.50248	6.50248	6.50248	6.50248	6.50248
	0.5	Present	3.67679	3.96622	4.10823	4.21479	4.40145	4.60566
		Present ($\kappa = 5/6$)	3.66392	3.95282	4.09653	4.20202	4.39016	4.59524
		Meiche et al.[30] (FSDT)	3.66866	3.95660	4.10007	4.20517	4.39336	4.59758
		Meiche et al.[30] (HSDT)	3.68219	3.97042	4.11235	4.21823	4.40499	4.60841
	1	Present	2.58239	2.91934	3.09595	3.23203	3.47425	3.75279
		Present ($\kappa = 5/6$)	2.57118	2.90690	3.08510	3.21946	3.46286	3.74182
		Meiche et al.[30] (FSDT)	2.57118	2.90690	3.08510	3.21946	3.46286	3.74182
		Meiche et al.[30] (HSDT)	2.58357	2.92003	3.09697	3.23237	3.47472	3.75328
	5	Present	1.32080	1.51412	1.69229	1.78553	2.05119	2.36523
		Present ($\kappa = 5/6$)	1.31925	1.51127	1.69271	1.77979	2.04643	2.35737
		Meiche et al.[30] (FSDT)	1.31921	1.51126	1.69269	1.77979	2.04642	2.35737
		Meiche et al.[30] (HSDT)	1.32910	1.52129	1.70176	1.78978	2.05605	2.36734
	10	Present	1.23333	1.36115	1.53014	1.58975	1.84504	2.13645
		Present ($\kappa = 5/6$)	1.23453	1.36311	1.53716	1.58760	1.84446	2.13022
		Meiche et al.[30] (FSDT)	1.23452	1.36313	1.53714	1.58760	1.84445	2.13020
		Meiche et al.[30] (HSDT)	1.24363	1.37316	1.54595	1.59736	1.85376	2.13995
Softcore	0	Present	1.19778	1.19778	1.19778	1.19778	1.19778	1.19778
		Present ($\kappa = 5/6$)	1.19778	1.19778	1.19778	1.19778	1.19778	1.19778
	0.5	Present	3.89577	3.57686	3.36321	3.33249	3.08599	2.97091
		Present ($\kappa = 5/6$)	4.00182	3.70663	3.47150	3.45643	3.18545	3.06736
	1	Present	4.92492	4.49483	4.19661	4.17322	3.82681	3.69711
		Present ($\kappa = 5/6$)	5.08266	4.73102	4.39634	4.41279	4.02034	3.89293
	5	Present	6.24287	5.71327	5.34656	5.34240	4.89413	4.78707
		Present ($\kappa = 5/6$)	6.35978	6.12612	5.71371	5.83195	5.30353	5.23756
	10	Present	6.38669	5.85661	5.50225	5.49520	5.04842	4.95318
		Present ($\kappa = 5/6$)	6.45714	6.28571	5.89109	6.03011	5.50129	5.46287

Table 8: Nondimensional critical buckling loads ($\bar{N}_{cr}$) of square Al/Al_2O_3 sandwich plates subjected to axial compression and tension ($R_1 = -1, R_2 = 1$) with homogeneous hardcore and softcore ($r = 2, s = 1$).

Core	p	Theory	$\bar{N}_{cr}$					
			1-0-1	2-1-2	2-1-1	1-1-1	2-2-1	1-2-1
Hardcore	0	Present	25.08395	25.08395	25.08395	25.08395	25.08395	25.08395
		Present ($\kappa = 5/6$)	25.08395	25.08395	25.08395	25.08395	25.08395	25.08395
	0.5	Present	14.49785	15.63207	16.16201	16.58767	17.28862	18.06726
		Present ($\kappa = 5/6$)	14.37837	15.50776	16.05379	16.46950	17.18448	17.97128
	1	Present	10.27527	11.61848	12.28950	12.83997	13.76415	14.84025
		Present ($\kappa = 5/6$)	10.16938	11.50089	12.18741	12.72160	13.65737	14.73777
	5	Present	5.24603	6.07759	6.76117	7.18544	8.22442	9.48400
		Present ($\kappa = 5/6$)	5.23139	6.05010	6.76521	7.12998	8.17865	9.40856
	10	Present	4.84684	5.43569	6.07595	6.38946	7.38868	8.58064
		Present ($\kappa = 5/6$)	4.85800	5.45449	6.14277	6.36871	7.38309	8.52064
Softcore	0	Present	4.62073	4.62073	4.62073	4.62073	4.62073	4.62073
		Present ($\kappa = 5/6$)	4.62073	4.62073	4.62073	4.62073	4.62073	4.62073
	0.5	Present	14.17523	12.82227	12.14688	11.90629	11.11902	10.65703
		Present ($\kappa = 5/6$)	15.04572	13.86644	13.02752	12.89777	11.92389	11.43060
	1	Present	17.85957	15.82706	14.89937	14.56184	13.48899	12.91515
		Present ($\kappa = 5/6$)	19.15293	17.69324	16.49581	16.42916	15.01788	14.43727
	5	Present	23.29657	19.87532	18.70071	18.11033	16.74805	16.06611
		Present ($\kappa = 5/6$)	24.29658	23.12874	21.61563	21.83897	19.90252	19.43169
	10	Present	24.16296	20.41769	19.25702	18.57307	17.20941	16.51246
		Present ($\kappa = 5/6$)	24.77655	23.81892	22.35563	22.64709	20.69369	20.30109

Table 9: The first three non-dimensional natural frequencies ($\bar{\omega}$) of (1-2-1) Al/Al_2O_3 sandwich plates with homogeneous hardcore and softcore.

Core	b/a	Mode (r,s)	Theory	p				
				0	0.5	1	5	10
Hardcore	0.5	1 (1,1)	Present	1.15479	0.99406	0.90788	0.73885	0.70645
			Present (κ=5/6)	1.15479	0.99336	0.90706	0.73809	0.70582
		2 (1,2)	Present	3.74119	3.24837	2.97893	2.44129	2.33612
			Present (κ=5/6)	3.74119	3.24131	2.97052	2.43337	2.32946
		3 (1,3)	Present	7.59854	6.67116	6.15153	5.08947	4.87567
			Present (κ=5/6)	7.59854	6.64373	6.11838	5.05746	4.84866
	1.0	1 (1,1)	Present	1.82442	1.57407	1.43927	1.17348	1.12226
			Present (κ=5/6)	1.82442	1.57234	1.43722	1.17159	1.12067
		2 (1,2)	Present	4.35246	3.78606	3.47539	2.85264	2.73025
			Present (κ=5/6)	4.35246	3.77659	3.46409	2.84196	2.72126
		3 (1,3)	Present	8.13770	7.15441	6.60202	5.46902	5.24005
			Present (κ=5/6)	8.13770	7.12320	6.56425	5.43242	5.20916
	2.0	1 (1,1)	Present	4.35246	3.78606	3.47539	2.85264	2.73025
			Present (κ=5/6)	4.35246	3.77659	3.46409	2.84196	2.72126
		2 (1,2)	Present	6.67896	5.84873	5.38697	4.44723	4.2593
			Present (κ=5/6)	6.67896	5.82725	5.36108	4.42237	4.23835
		3 (1,3)	Present	10.20908	9.02134	8.34710	6.94674	6.65959
			Present (κ=5/6)	10.20908	8.97372	8.28906	6.88982	6.61148
Softcore	0.5	1 (1,1)	Present	0.58723	0.90459	0.99774	1.10940	1.12247
			Present (κ=5/6)	0.58723	0.91382	1.01431	1.14192	1.15837
		2 (1,2)	Present	1.90245	2.82533	3.07379	3.34643	3.37378
			Present (κ=5/6)	1.90245	2.90906	3.22063	3.62579	3.68104
		3 (1,3)	Present	3.86398	5.49440	5.88934	6.27608	6.30548
			Present (κ=5/6)	3.86398	5.78299	6.38268	7.18600	7.30254
	1.0	1 (1,1)	Present	0.92775	1.41475	1.55414	1.71736	1.73573
			Present (κ=5/6)	0.92775	1.43687	1.59360	1.79408	1.82035
		2 (1,2)	Present	2.21330	3.26211	3.53910	3.83753	3.86632
			Present (κ=5/6)	2.21330	3.37201	3.73087	4.20024	4.26497
		3 (1,3)	Present	4.13815	6.12408	6.61530	7.13333	7.18349
			Present (κ=5/6)	4.13815	6.17714	6.81492	7.67274	7.79808
	2.0	1 (1,1)	Present	2.21330	3.26211	3.53910	3.83753	3.86632
			Present (κ=5/6)	2.21330	3.37201	3.73087	4.20024	4.26497
		2 (1,2)	Present	3.39636	4.87565	5.24173	5.61023	5.64041
			Present (κ=5/6)	3.39636	5.10773	5.64044	6.35024	6.45188
		3 (1,3)	Present	5.19148	7.20674	7.66527	8.08358	8.10812
			Present (κ=5/6)	5.19148	7.67627	8.45719	9.52217	9.68176

Table 10: Nondimensional critical buckling loads ($\bar{N}_{cr}$) of (1-2-1) Al/Al_2O_3 sandwich plates with homogeneous hardcore and softcore.

Core	(R_1, R_2)	b/a	Theory	p				
				0	0.5	1	5	10
Hardcore	(-1, 0)	0.5[a]	Present	52.01795	36.84532	30.02233	18.92183	17.09157
			Present (κ=5/6)	52.01795	36.76190	29.93460	18.85898	17.04178
		1.0	Present	13.00449	9.21133	7.50558	4.73046	4.27289
			Present (κ=5/6)	13.00449	9.19048	7.48365	4.71474	4.26044
		2.0	Present	4.70324	3.38761	2.78255	1.77825	1.60887
			Present (κ=5/6)	4.70324	3.36962	2.76333	1.76411	1.59762
	(-1, -1)	0.5	Present	16.5877	11.69721	9.50956	5.97149	5.39158
			Present (κ=5/6)	16.5877	11.68038	9.49193	5.95896	5.38166
		1.0	Present	6.50224	4.60566	3.75279	2.36523	2.13645
			Present (κ=5/6)	6.50224	4.59524	3.74182	2.35737	2.13022
		2.0	Present	3.76259	2.71009	2.22604	1.42260	1.28710
			Present (κ=5/6)	3.76259	2.69569	2.21067	1.41128	1.27810
	(-1, 1)	0.5	Present	27.64616	19.49535	15.84926	9.95248	8.98596
			Present (κ=5/6)	27.64616	19.46730	15.81989	9.93159	8.96943
		1.0[a]	Present	25.08395	18.06726	14.84025	9.48400	8.58064
			Present (κ=5/6)	25.08395	17.97128	14.73777	9.40856	8.52064
		2.0	Present	6.27099	4.51681	3.71006	2.37100	2.14516
			Present (κ=5/6)	6.27099	4.49282	3.68444	2.35214	2.13016
Softcore	(-1, 0)	0.5[a]	Present	9.58225	23.76728	29.57688	38.29658	39.62548
			Present (κ=5/6)	9.58225	24.53887	31.14342	41.90052	43.70299
		1.0	Present	2.39556	5.94182	7.39422	9.57415	9.90637
			Present (κ=5/6)	2.39556	6.13472	7.78586	10.4751	10.92575
		2.0	Present	0.86639	1.99819	2.42159	3.01240	3.09609
			Present (κ=5/6)	0.86639	2.14324	2.70699	3.64344	3.80645
	(-1, -1)	0.5	Present	3.05563	7.73871	9.71073	12.73667	13.20800
			Present (κ=5/6)	3.05563	7.90048	10.04242	13.50957	14.08400
		1.0	Present	1.19778	2.97091	3.69711	4.78707	4.95318
			Present (κ=5/6)	1.19778	3.06736	3.89293	5.23756	5.46287
		2.0	Present	0.69311	1.59856	1.93727	2.40992	2.47687
			Present (κ=5/6)	0.69311	1.71459	2.16559	2.91475	3.04516
	(-1, 1)	0.5	Present	5.09271	12.89784	16.18454	21.22778	22.01334
			Present (κ=5/6)	5.09271	13.16746	16.73737	22.51595	23.47333
		1.0[a]	Present	4.62073	10.65703	12.91515	16.06611	16.51246
			Present (κ=5/6)	4.62073	11.43060	14.43727	19.43169	20.30109
		2.0	Present	1.15518	2.66426	3.22879	4.01653	4.12812
			Present (κ=5/6)	1.15518	2.85765	3.60932	4.85792	5.07527

(a) : Critical buckling occurs at $(r, s) = (2, 1)$.

Table 11: The first three non-dimensional natural frequencies ($\bar{\omega}$) of (1-2-1) Al/SiC sandwich plates with homogeneous hardcore and softcore.

Core	b/a	Mode (r,s)	Theory	p				
				0	0.5	1	5	10
Hardcore	0.5	1 (1,1)	Present	1.32091	1.11899	1.01214	0.80376	0.76356
			Present (κ=5/6)	1.32091	1.11819	1.01123	0.80297	0.76291
		2 (1,2)	Present	4.27939	3.65629	3.32058	2.65537	2.52463
			Present (κ=5/6)	4.27939	3.64829	3.31126	2.64712	2.51786
		3 (1,3)	Present	8.69165	7.50826	6.85610	5.53487	5.26839
			Present (κ=5/6)	8.69165	7.47722	6.81944	5.50157	5.24096
	1.0	1 (1,1)	Present	2.08688	1.77185	1.60449	1.27653	1.21294
			Present (κ=5/6)	2.08688	1.76988	1.60222	1.27454	1.21131
		2 (1,2)	Present	4.97860	4.26142	3.87388	3.10270	2.95050
			Present (κ=5/6)	4.97860	4.25069	3.86136	3.09157	2.94135
		3 (1,3)	Present	9.30838	8.05208	7.35809	5.94753	5.66204
			Present (κ=5/6)	9.30838	8.01677	7.31631	5.90946	5.63067
	2.0	1 (1,1)	Present	4.97860	4.26142	3.87388	3.10270	2.95050
			Present (κ=5/6)	4.97860	4.25069	3.86136	3.09157	2.94135
		2 (1,2)	Present	7.63979	6.58272	6.00413	4.83658	4.60251
			Present (κ=5/6)	7.63979	6.55840	5.97549	4.81071	4.58121
		3 (1,3)	Present	11.67773	10.15303	9.30262	7.55408	7.19555
			Present (κ=5/6)	11.67773	10.09916	9.23848	7.49495	7.14674
Softcore	0.5	1 (1,1)	Present	0.58723	0.95454	1.06566	1.20657	1.22500
			Present (κ=5/6)	0.58723	0.96585	1.08612	1.24721	1.27001
		2 (1,2)	Present	1.90245	2.97009	3.26637	3.61336	3.65396
			Present (κ=5/6)	1.90245	3.07211	3.44638	3.95904	4.03498
		3 (1,3)	Present	3.86398	5.75131	6.22421	6.72857	6.77860
			Present (κ=5/6)	3.86398	6.10050	6.82391	7.84277	8.00164
	1.0	1 (1,1)	Present	0.92775	1.49127	1.65750	1.86377	1.88996
			Present (κ=5/6)	0.92775	1.51835	1.70613	1.95938	1.99569
		2 (1,2)	Present	2.21330	3.42664	3.75705	4.13800	4.18145
			Present (κ=5/6)	2.21330	3.56037	3.99178	4.58595	4.67480
		3 (1,3)	Present	4.13815	6.12408	6.61530	7.13333	7.18349
			Present (κ=5/6)	4.13815	6.51538	7.28517	8.37341	8.54413
	2.0	1 (1,1)	Present	2.21330	3.42664	3.75705	4.13800	4.18145
			Present (κ=5/6)	2.21330	3.56037	3.99178	4.58595	4.67480
		2 (1,2)	Present	3.39636	5.10827	5.54607	6.02332	6.07261
			Present (κ=5/6)	3.39636	5.38950	6.03160	6.93142	7.07022
		3 (1,3)	Present	5.19148	7.52656	8.07852	8.63683	8.68587
			Present (κ=5/6)	5.19148	8.09248	9.03679	10.3890	10.6056

Table 12: Nondimensional critical buckling load ($\bar{N}_{cr}$) of (1-2-1) Al/SiC sandwich plates with homogeneous hardcore and softcore.

Core	(R_1, R_2)	b/a	Theory	p				
				0	0.5	1	5	10
Hardcore	(-1, 0)	0.5[a]	Present	57.49352	40.35869	32.65022	20.10553	18.03736
			Present (κ=5/6)	57.49352	40.26658	32.55521	20.04133	17.98770
		1.0	Present	14.37338	10.08967	8.16256	5.02638	4.50934
			Present (κ=5/6)	14.37338	10.06665	8.13880	5.01033	4.49693
		2.0	Present	5.19832	3.71202	3.02782	1.89138	1.69976
			Present (κ=5/6)	5.19832	3.69214	3.00699	1.87690	1.68851
	(-1, -1)	0.5	Present	18.33377	12.81134	10.34038	6.34339	5.68830
			Present (κ=5/6)	18.33377	12.79276	10.32130	6.33059	5.67841
		1.0	Present	7.18669	5.04484	4.08128	2.51319	2.25467
			Present (κ=5/6)	7.18669	5.03332	4.06940	2.50517	2.24846
		2.0	Present	4.15866	2.96962	2.42226	1.51310	1.35981
			Present (κ=5/6)	4.15866	2.95371	2.40559	1.50152	1.35081
	(-1, 1)	0.5	Present	30.55628	21.35223	17.23396	10.57232	9.48050
			Present (κ=5/6)	30.55628	21.32127	17.20216	10.55099	9.46402
		1.0[a]	Present	27.72437	19.79747	16.14838	10.08735	9.06537
			Present (κ=5/6)	27.72437	19.69142	16.03726	10.01013	9.00540
		2.0	Present	6.93109	4.94937	4.03709	2.52184	2.26634
			Present (κ=5/6)	6.93109	4.92285	4.00932	2.50253	2.25135
Softcore	(-1, 0)	0.5[a]	Present	9.58225	25.49135	31.94771	41.55328	43.00124
			Present (κ=5/6)	9.58225	26.45206	33.90385	46.0497	48.08656
		1.0	Present	2.39556	6.37284	7.98693	10.38832	10.75031
			Present (κ=5/6)	2.39556	6.61302	8.47596	11.51243	12.02164
		2.0	Present	0.86639	2.12623	2.58868	3.22291	3.31064
			Present (κ=5/6)	0.86639	2.30498	2.94062	3.99803	4.18239
	(-1, -1)	0.5	Present	3.05563	8.32005	10.52354	13.88475	14.40457
			Present (κ=5/6)	3.05563	8.52209	10.93935	14.85403	15.50296
		1.0	Present	1.19778	3.18642	3.99346	5.19416	5.37516
			Present (κ=5/6)	1.19778	3.30651	4.23798	5.75621	6.01082
		2.0	Present	0.69311	1.70098	2.07094	2.57833	2.64851
			Present (κ=5/6)	0.69311	1.84399	2.35249	3.19842	3.34591
	(-1, 1)	0.5	Present	5.09271	13.86674	17.53923	23.14126	24.00761
			Present (κ=5/6)	5.09271	14.20348	18.23225	24.75672	25.83827
		1.0[a]	Present	4.62073	11.33988	13.80628	17.18885	17.65676
			Present (κ=5/6)	4.62073	12.29324	15.68328	21.32283	22.30607
		2.0	Present	1.15518	2.83497	3.45157	4.29721	4.41419
			Present (κ=5/6)	1.15518	3.07331	3.92082	5.33071	5.57652

(a) : Critical buckling occurs at $(r, s) = (2, 1)$.

Table 13: The first three non-dimensional natural frequencies ($\bar{\omega}$) of (1-2-1) Al/WC sandwich plates with homogeneous hardcore and softcore.

Core	b/a	Mode (r,s)	Theory	p				
				0	0.5	1	5	10
Hardcore	0.5	1 (1,1)	Present	0.76864	0.68054	0.62849	0.51503	0.49181
			Present (κ=5/6)	0.76864	0.68004	0.62794	0.51462	0.49150
		2 (1,2)	Present	2.49017	2.22861	2.06914	1.71207	1.63717
			Present (κ=5/6)	2.49017	2.22356	2.06343	1.70768	1.63383
		3 (1,3)	Present	5.05767	4.58909	4.29138	3.59900	3.44849
			Present (κ=5/6)	5.05767	4.56930	4.26847	3.58060	3.43439
	1.0	1 (1,1)	Present	1.21435	1.07824	0.99726	0.81931	0.78266
			Present (κ=5/6)	1.21435	1.07701	0.99588	0.81828	0.78188
		2 (1,2)	Present	2.89704	2.59867	2.41576	2.00330	1.91629
			Present (κ=5/6)	2.89704	2.59190	2.40806	1.99734	1.91174
		3 (1,3)	Present	5.41654	4.92312	4.60818	3.87163	3.71073
			Present (κ=5/6)	5.41654	4.90058	4.58201	3.85049	3.69452
	2.0	1 (1,1)	Present	2.89704	2.59867	2.41576	2.00330	1.91629
			Present (κ=5/6)	2.89704	2.59190	2.40806	1.99734	1.91174
		2 (1,2)	Present	4.44559	4.02093	3.75439	3.13887	3.00619
			Present (κ=5/6)	4.44559	4.00546	3.73656	3.12469	2.99534
		3 (1,3)	Present	6.79527	6.21509	5.83782	4.93765	4.73732
			Present (κ=5/6)	6.79527	6.18052	5.79729	4.90423	4.71160
Softcore	0.5	1 (1,1)	Present	0.58723	0.87379	0.90143	0.89350	0.88371
			Present (κ=5/6)	0.58723	0.89458	0.93523	0.95048	0.94498
		2 (1,2)	Present	1.90245	2.64295	2.66487	2.55119	2.50780
			Present (κ=5/6)	1.90245	2.81948	2.94153	2.99574	2.98254
		3 (1,3)	Present	3.86398	4.97548	4.90944	4.56159	4.46182
			Present (κ=5/6)	3.86398	5.54532	5.77228	5.89245	5.87552
	1.0	1 (1,1)	Present	0.92775	1.35372	1.38675	1.35964	1.34209
			Present (κ=5/6)	0.92775	1.40261	1.46532	1.49010	1.48206
		2 (1,2)	Present	2.21330	3.03296	3.04513	2.89782	2.84563
			Present (κ=5/6)	2.21330	3.26177	3.40126	3.46541	3.45111
		3 (1,3)	Present	4.13815	5.28158	5.19926	4.81619	4.70855
			Present (κ=5/6)	4.13815	5.91613	6.15642	6.28633	6.26939
	2.0	1 (1,1)	Present	2.21330	3.03296	3.04513	2.89782	2.84563
			Present (κ=5/6)	2.21330	3.26177	3.40126	3.46541	3.45111
		2 (1,2)	Present	3.39636	4.44440	4.40367	4.11506	4.02877
			Present (κ=5/6)	3.39636	4.90874	5.11129	5.21511	5.19845
		3 (1,3)	Present	5.19148	6.42302	6.27346	5.75318	5.61569
			Present (κ=5/6)	5.19148	7.32145	7.61144	7.77964	7.76355

Table 14: Nondimensional critical buckling load ($\bar{N}_{cr}$) of (1-2-1) Al/WC sandwich plates with homogeneous hardcore and softcore.

Core	(R_1, R_2)	b/a	Theory	p				
				0	0.5	1	5	10
Hardcore	(-1, 0)	0.5[a]	Present	95.82254	64.94925	51.03866	28.37511	24.64075
			Present (κ=5/6)	95.82254	64.79755	50.89483	28.30233	24.59067
		1.0	Present	23.95563	16.23731	12.75967	7.09378	6.16019
			Present (κ=5/6)	23.95563	16.19939	12.72371	7.07558	6.14767
		2.0	Present	8.66387	5.98230	4.74329	2.67967	2.33217
			Present (κ=5/6)	8.66387	5.94945	4.71162	2.66312	2.32072
	(-1, -1)	0.5	Present	30.55628	20.60965	16.15474	8.94343	7.76193
			Present (κ=5/6)	30.55628	20.57908	16.12589	8.92896	7.75198
		1.0	Present	11.97782	8.11866	6.37983	3.54689	3.08009
			Present (κ=5/6)	11.97782	8.09969	6.36185	3.53779	3.07383
		2.0	Present	6.93109	4.78584	3.79464	2.14374	1.86574
			Present (κ=5/6)	6.93109	4.75956	3.76929	2.13049	1.85658
	(-1, 1)	0.5	Present	50.92714	34.34942	26.92457	14.90572	12.93655
			Present (κ=5/6)	50.92714	34.29846	26.87648	14.88159	12.91997
		1.0[a]	Present	46.20728	31.90558	25.29757	14.29159	12.43826
			Present (κ=5/6)	46.20728	31.73043	25.12862	14.20328	12.37718
		2.0	Present	11.55182	7.97640	6.32439	3.57290	3.10957
			Present (κ=5/6)	11.55182	7.93261	6.28215	3.55082	3.09430
Softcore	(-1, 0)	0.5[a]	Present	9.58225	36.97288	47.42629	62.07606	64.11738
			Present (κ=5/6)	9.58225	39.80326	53.18593	75.06686	78.74836
		1.0	Present	2.39556	9.24322	11.85657	15.51902	16.02934
			Present (κ=5/6)	2.39556	9.95082	13.29648	18.76671	19.68709
		2.0	Present	0.86639	2.93453	3.60597	4.42878	4.52436
			Present (κ=5/6)	0.86639	3.43013	4.56906	6.47551	6.80994
	(-1, -1)	0.5	Present	3.05563	12.25796	15.95509	21.36900	22.16413
			Present (κ=5/6)	3.05563	12.86453	17.20899	24.25939	25.43073
		1.0	Present	1.19778	4.62161	5.92829	7.75951	8.01467
			Present (κ=5/6)	1.19778	4.97541	6.64824	9.38336	9.84355
		2.0	Present	0.69311	2.34762	2.88477	3.54302	3.61949
			Present (κ=5/6)	0.69311	2.74410	3.65525	5.18041	5.44795
	(-1, 1)	0.5	Present	5.09271	20.42993	26.59182	35.61500	36.94022
			Present (κ=5/6)	5.09271	21.44089	28.68166	40.43232	42.38456
		1.0[a]	Present	4.62073	15.65081	19.23181	23.62015	24.12991
			Present (κ=5/6)	4.62073	18.29401	24.36830	34.53606	36.31966
		2.0	Present	1.15518	3.91270	4.80795	5.90504	6.03248
			Present (κ=5/6)	1.15518	4.57350	6.09208	8.63401	9.07992

(a) : Critical buckling occurs at $(r, s) = (2, 1)$.